Gravitational waves from small mass-ratio binaries

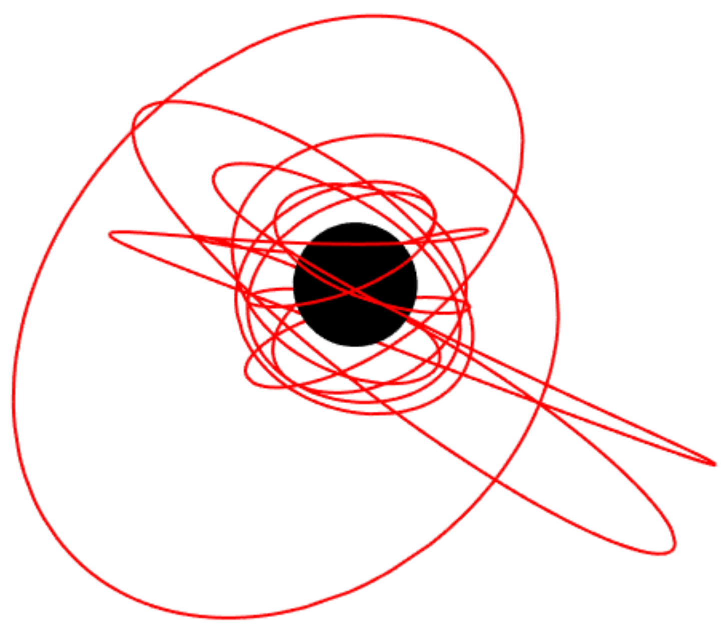

Niels Warburton

Royal Society - SFI University Research Fellow

University College Dublin

IV Mesoamerican Workshop
On Cosmology and Gravitation
10th November 2020

Thanks for the invitation

(I miss the amazing food in Mexico)

Tacos al Pastor in Coyoacán with
C. Lopez Monsalvo in 2015

Overview

Gravitational waves from small mass-ratio binaries

- Motivation: GW observations, IMBHs, EMRIs
- Status of modelling black hole binaries
- Non-linear black hole perturbation theory
- New results that shed light on what counts as ‘small’?

Why are we interested in small mass-ratio binaries?

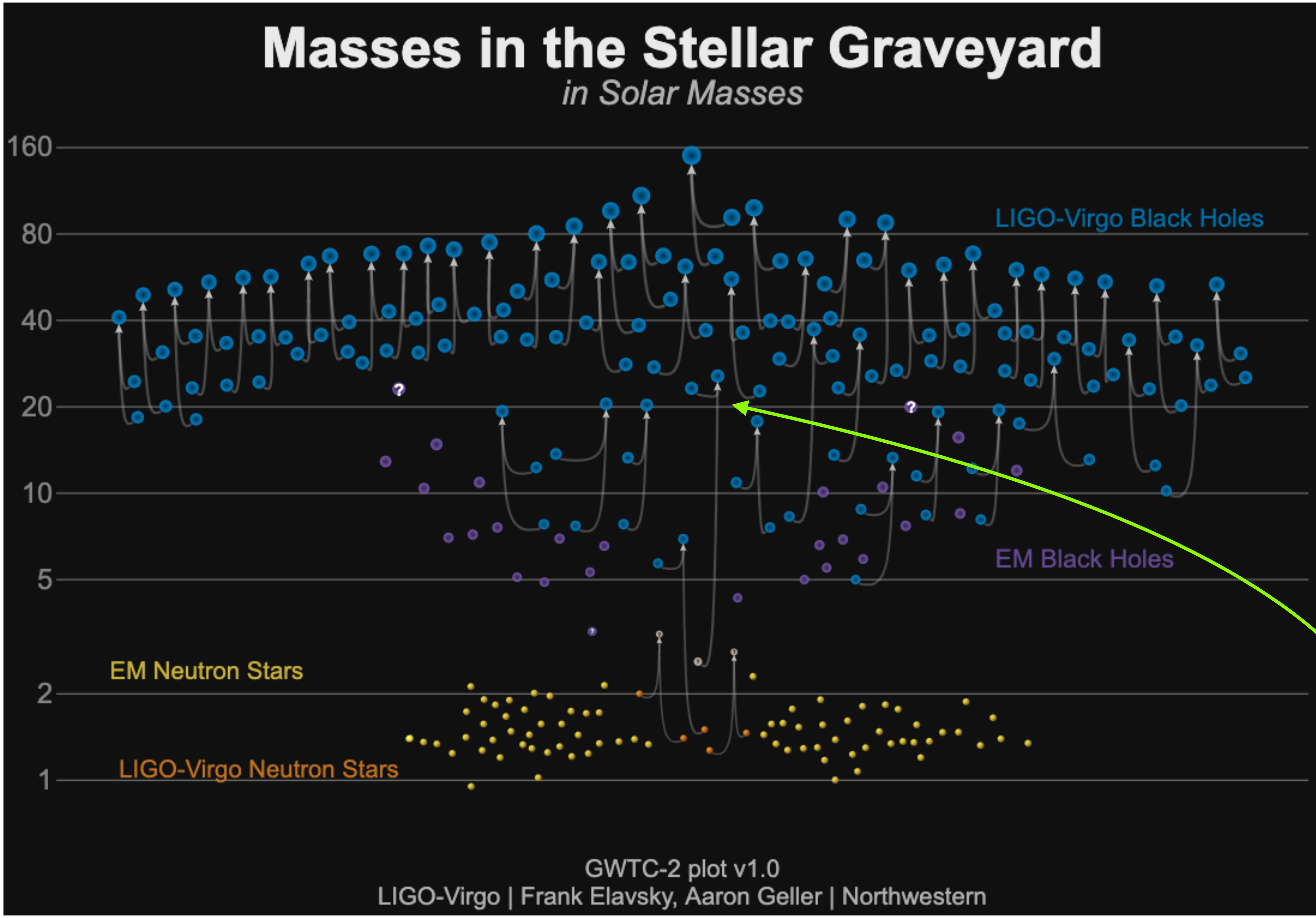

GW190814: merger of 23 $M_{\odot}$ black hole with a 2.6 $M_{\odot}$ compact object

Mass ratio of ~ 9:1. Is this a small mass-ratio binary?

Why are we interested in small mass-ratio binaries?

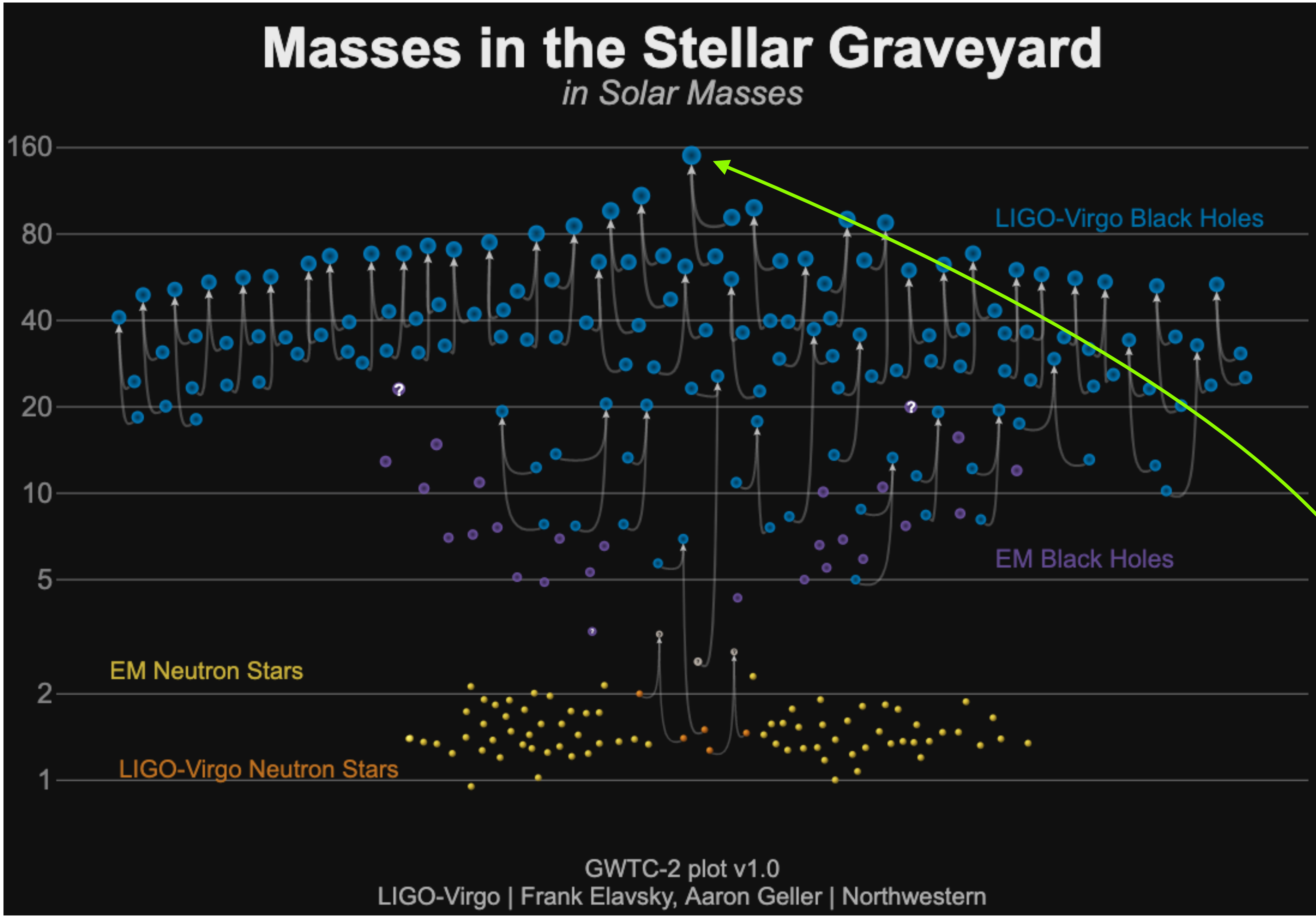

GW190521: a binary black hole (BBH) with total mass 150 $M_\odot$

The first confirmed detection of an intermediate-mass black hole

Why are we interested in small mass-ratio binaries?

With IMBHs confirmed to exist, this raises the possibility of intermediate mass-ratio inspirals (IMRIs). These are binaries with mass-ratios in the range of $10^2 - 10^4 : 1$

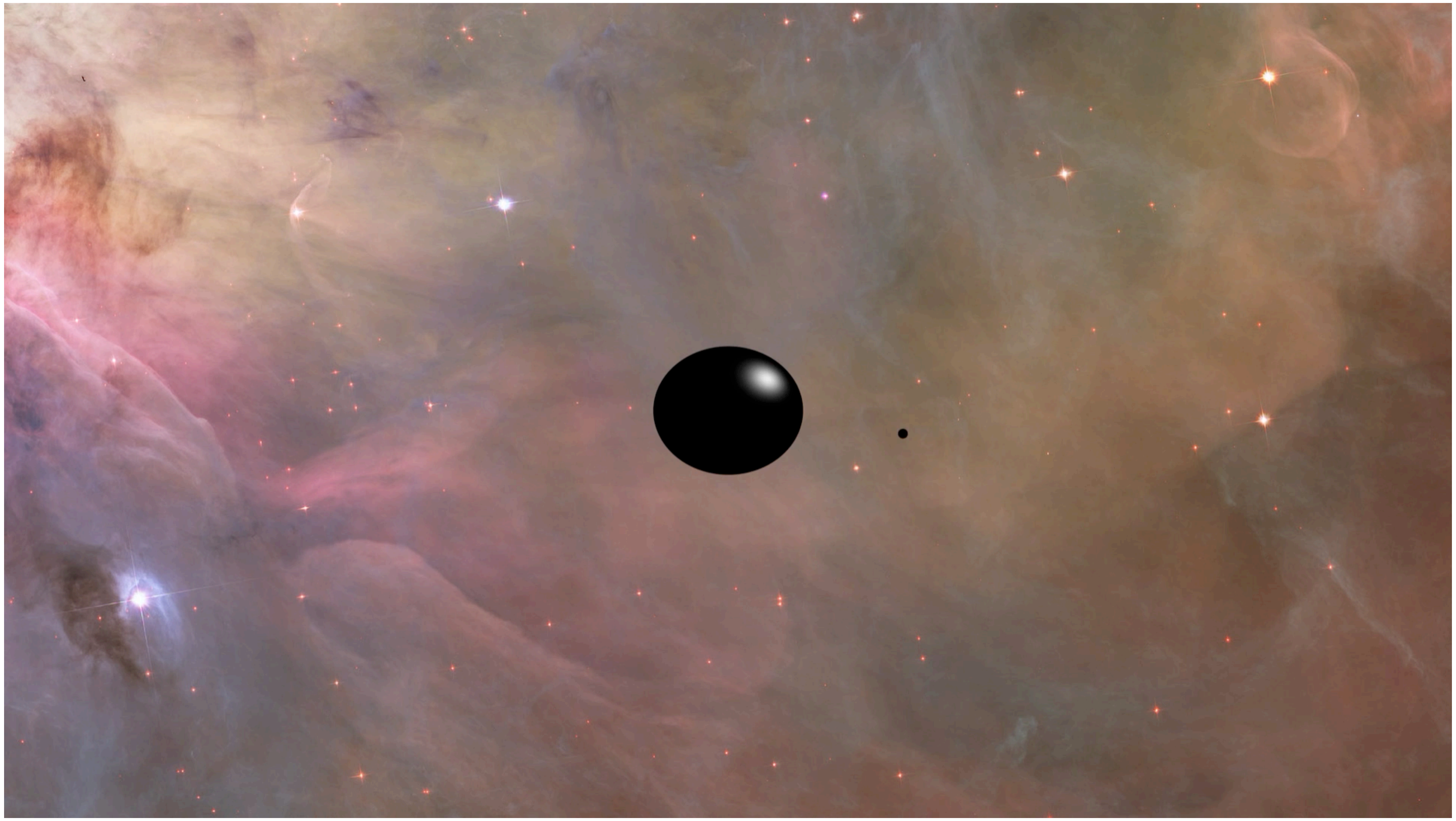

Simulation (by Steve Drasco) of 2000:1 mass-ratio binary where the primary has a mass of $3000 M_\odot$ and the secondary has the mass of a neutron star.

Why are we interested in small mass-ratio binaries?

We can also have stellar-mass compact objects falling onto a massive black hole.
These binaries are called extreme mass-ratio inspirals (EMRIs)

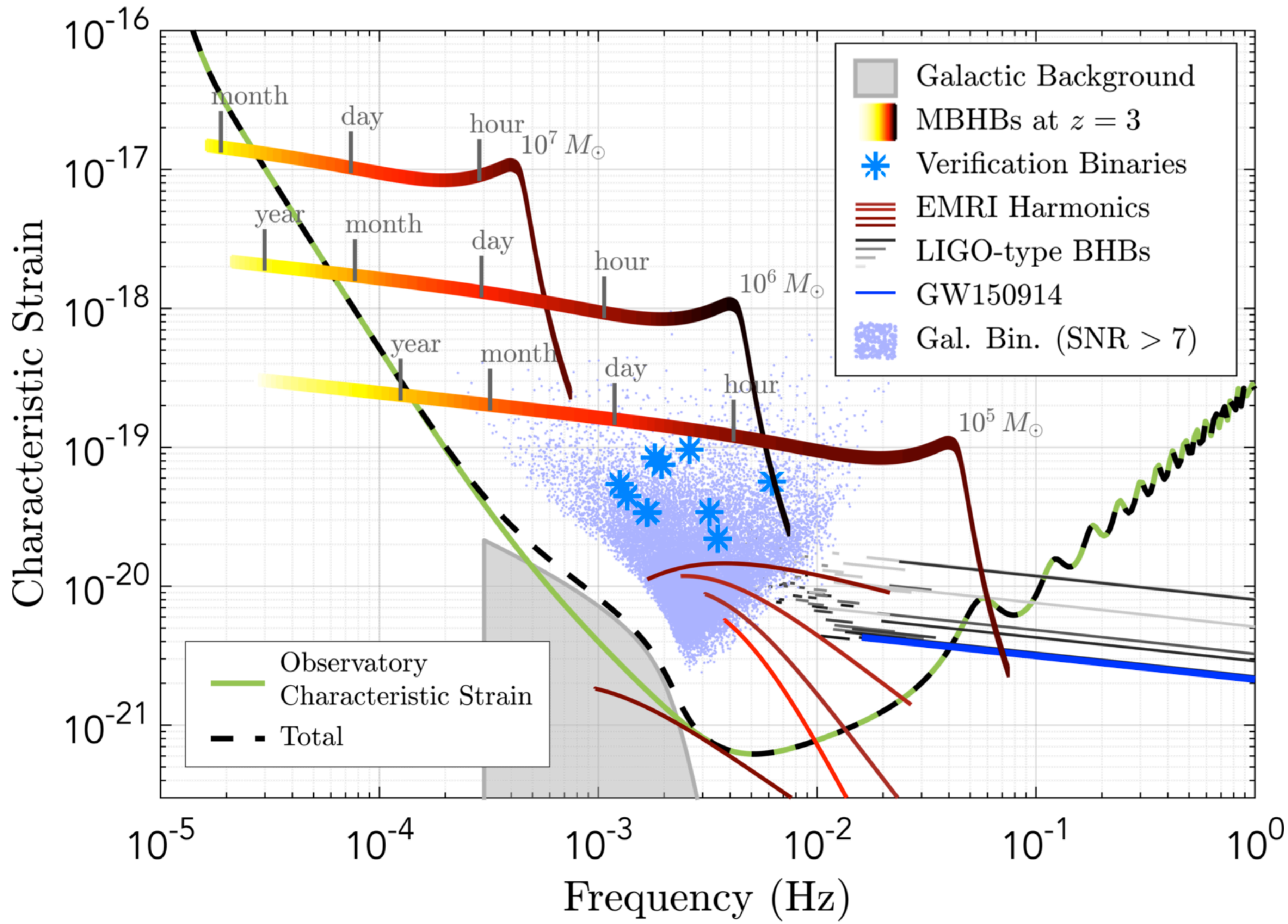

EMRIs are a key source for LISA

Extreme mass-ratio inspirals

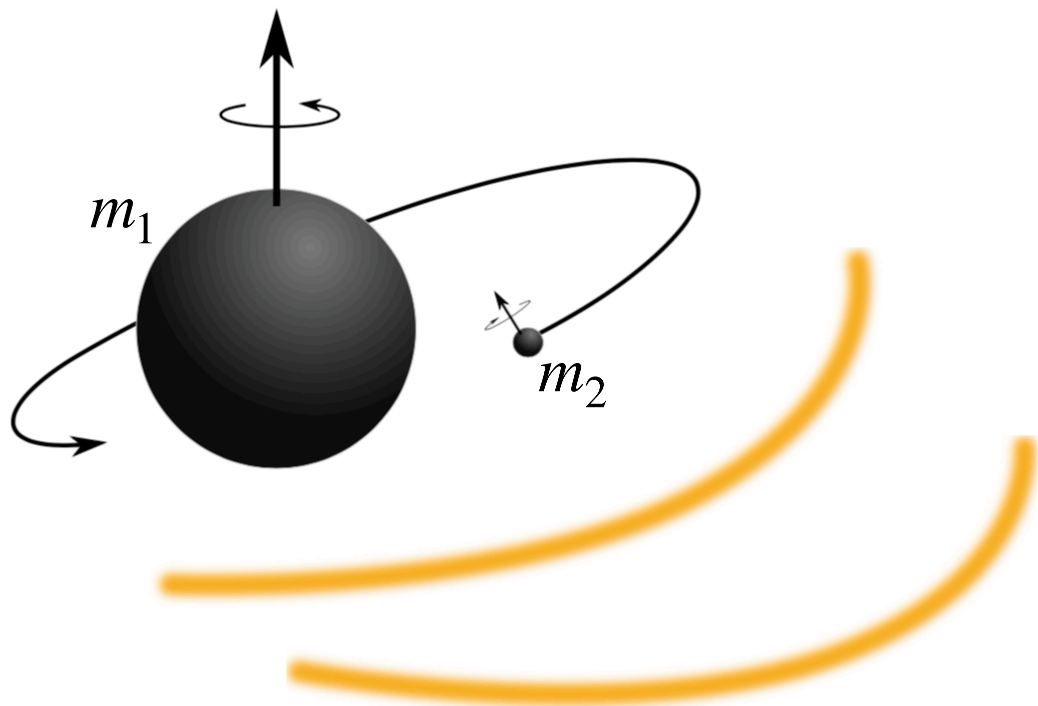

Image credit: A. Pound

- Binary with an extremely small mass ratio $\epsilon = m_2/m_1 \ll 1$
- Primary: massive black hole
- Secondary: compact object such as a stellar-mass black hole, neutron star
- For LISA EMRIs: $\epsilon = 10^{-4}$-10^{-7}

Key Features:

- Millihertz gravitational-wave source
- Over 100,000+ orbits in strong field
- Visible for months to years in LISA band
- No spin alignment expected
- Considerable eccentricity
- Rich waveform phenomenology
- Very low instantaneous SNR in LISA

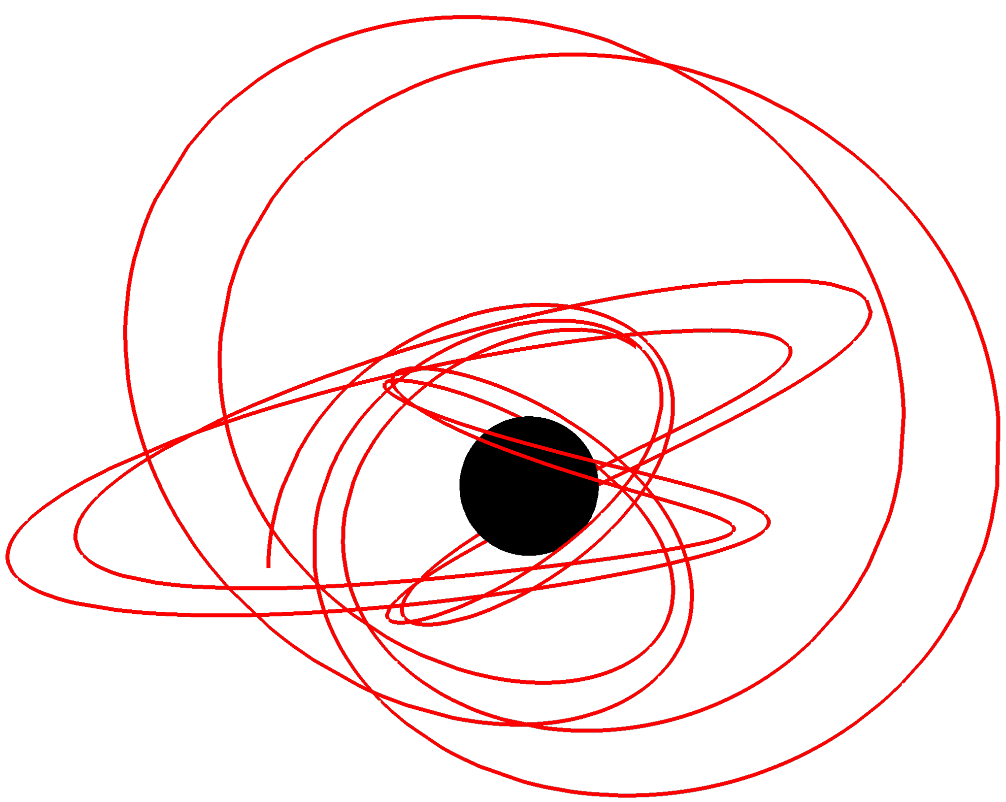

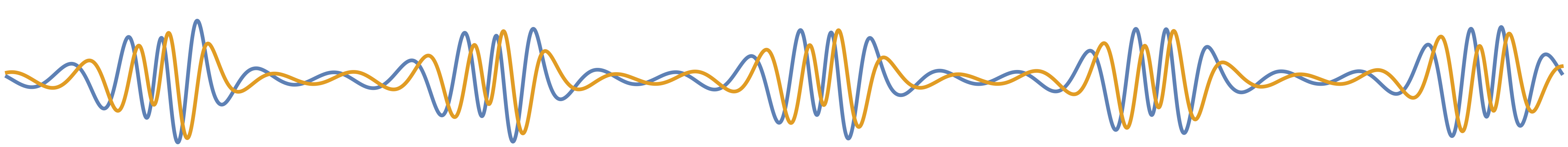

Approaches to modelling the two-body problem

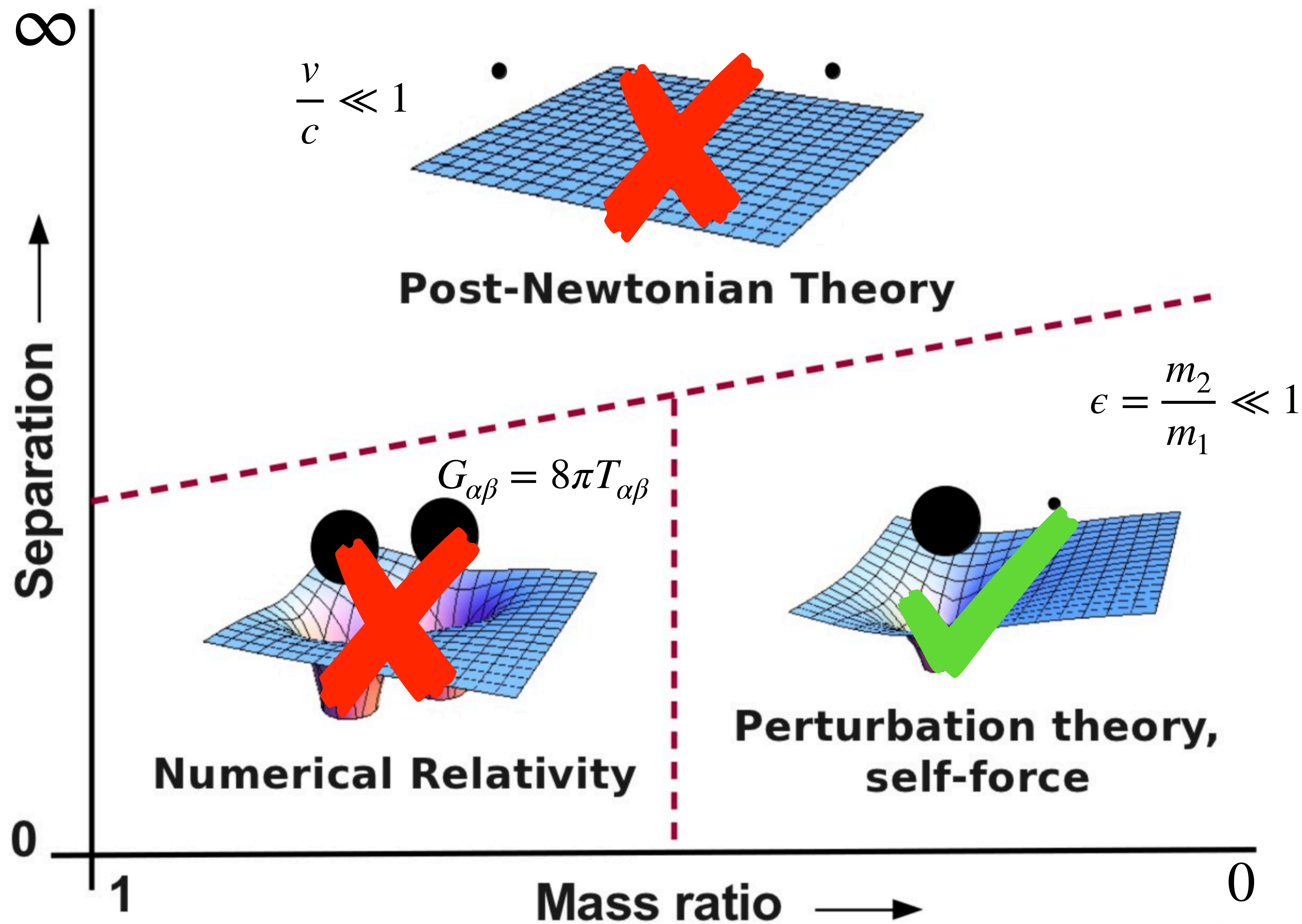

Credit: Leor Barack

Coverage of numerical relativity waveforms

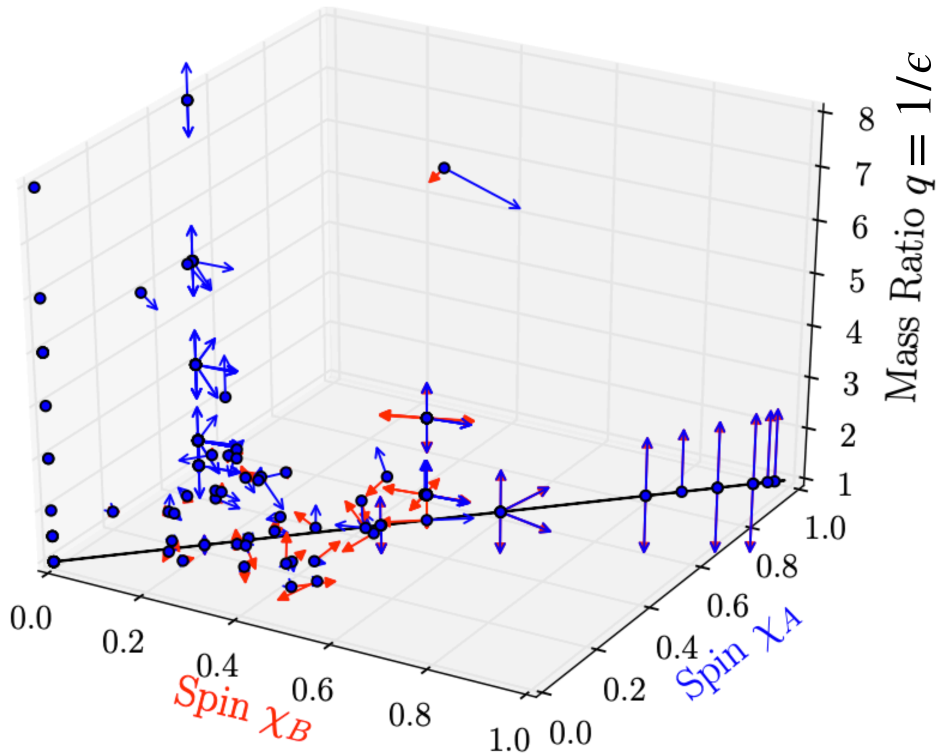

174 BBHs in SXS 2013 catalogue

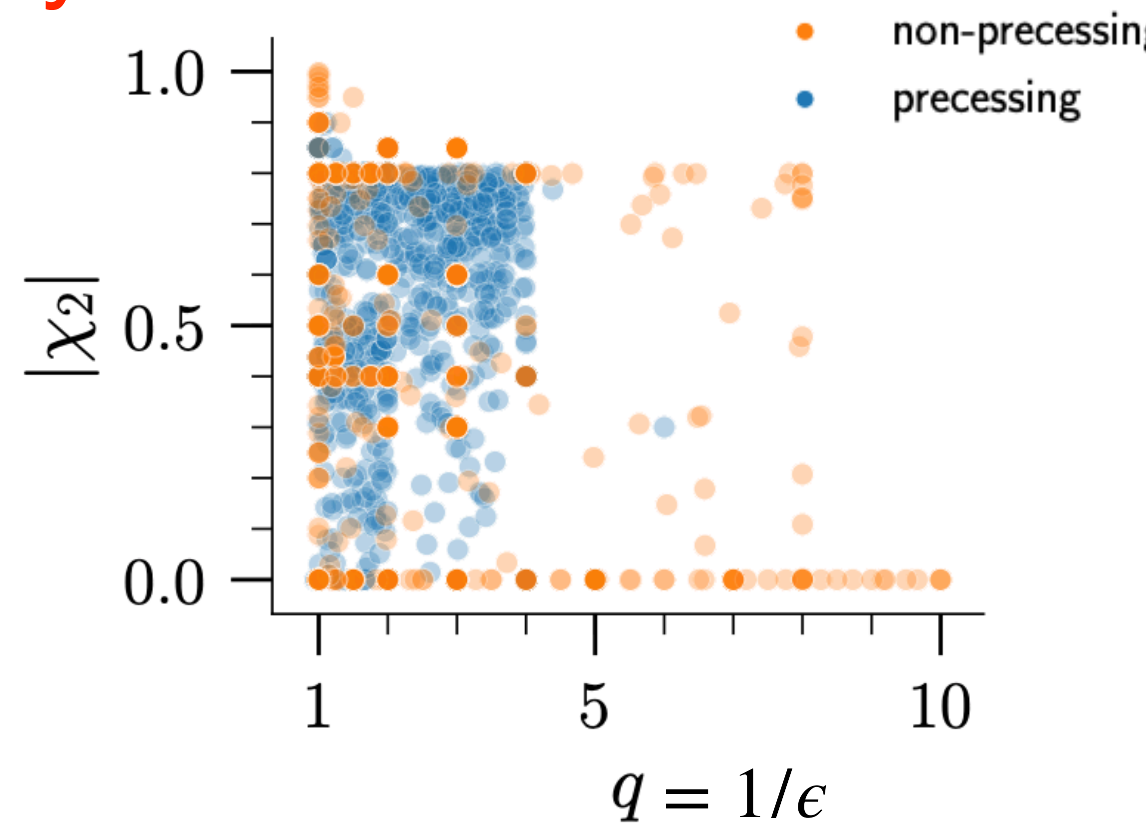

~ 2000 BBHs in SXS 2019 catalogue

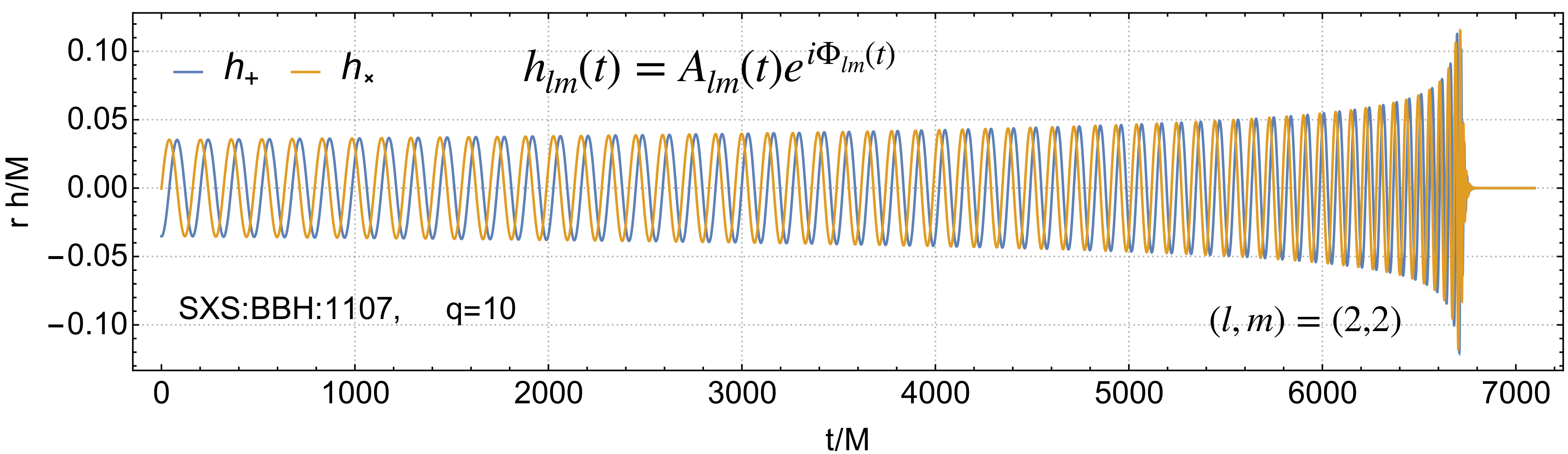

A NR waveform like above has ~40 cycles and takes months to compute on a supercomputer with hundreds of processing cores

Black Hole Perturbation Theory

Use mass ratio, $\epsilon = m_2/m_1$, as an expansion parameter and expand the metric of the binary about the metric of the primary

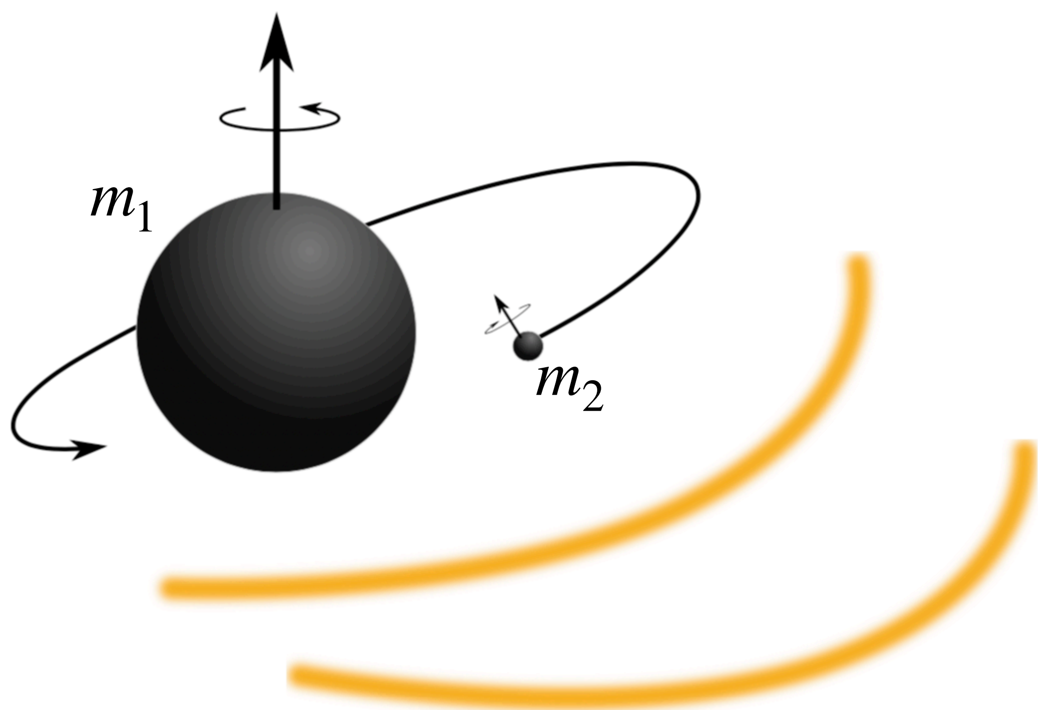

Image credit: A. Pound

$$g_{\alpha\beta} = \bar{g}_{\alpha\beta} + \epsilon h^{(1)}_{\alpha\beta} + \epsilon^2 h^{(2)}_{\alpha\beta} + \mathcal{O}(\epsilon^3)$$

Schwarzschild or Kerr

Model secondary as a point particle

$$T_{\alpha\beta} = m_2 \int_{\infty}^{\infty} |\bar{g}|^{-1/2} \delta^4(x^\mu - z^\mu) u_\alpha u_\beta \, d\tau$$

Substitute into the Einstein equation $G_{\alpha\beta}[g] = 8\pi T_{\alpha\beta}$ and expand order-by-order

Equations of motion: $u^\beta \nabla_\beta u^\alpha = F^\alpha_{self}[h; z]$

Self-force

Black Hole Perturbation Theory

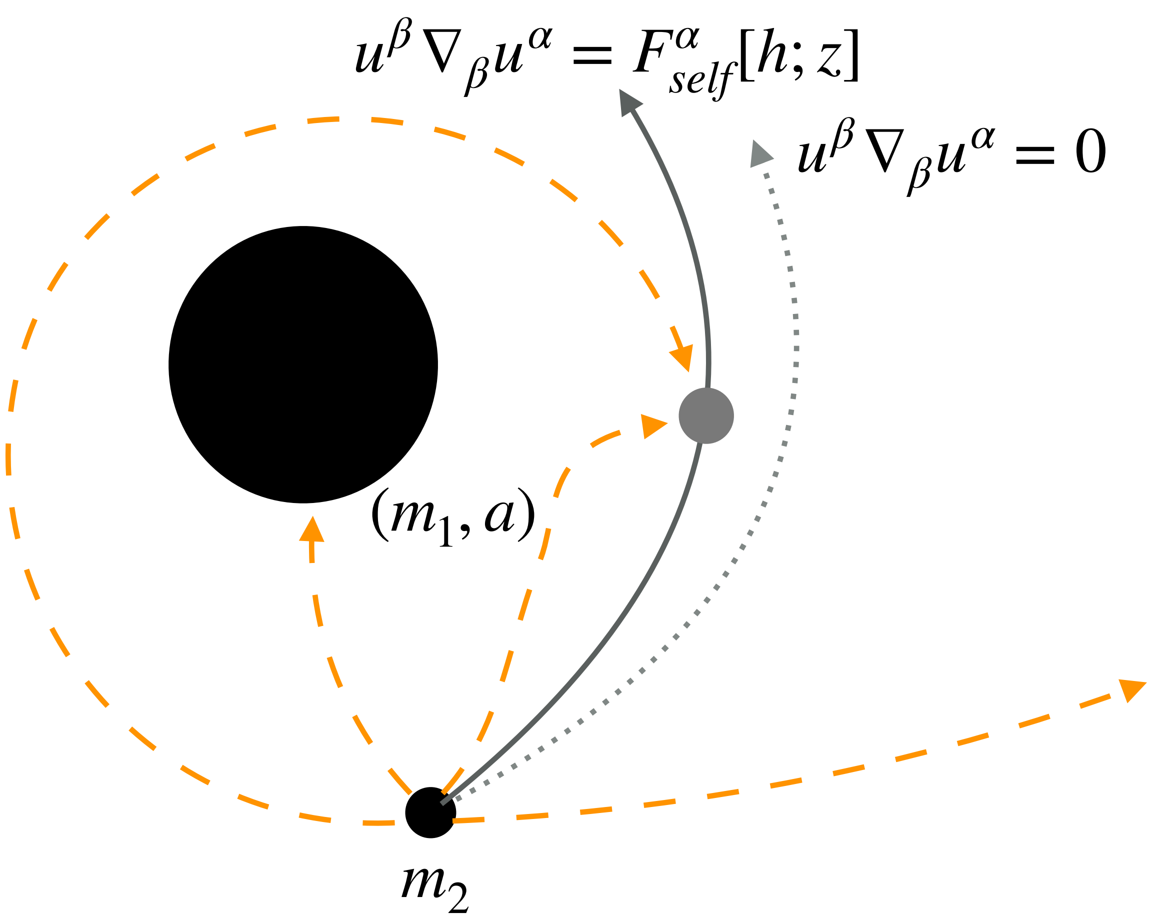

The force at a given instance depends upon the local metric perturbation, which is a functional of the entire past history of the particle

Light cone about field point x^μ

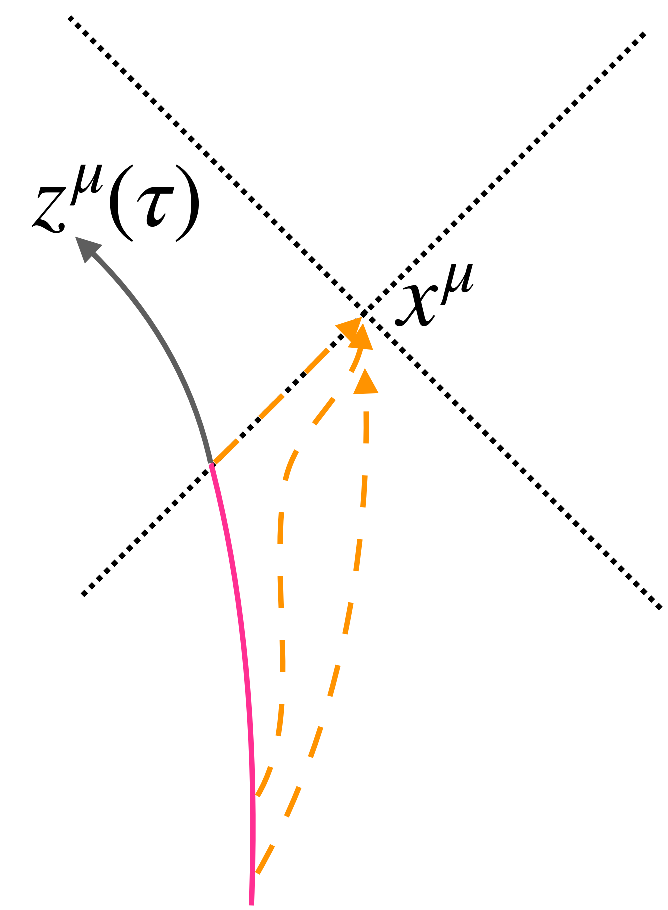

$$F^\alpha_{self}[z_\mu(\tau)] = \lim_{x^\mu \to z^\mu(\tau)} F[\nabla^\alpha h(x^\mu)]$$

As defined here, this diverges in the limit. Thus we need to regularize

Defining the self-force: regular/singular split

Regularization precisely defined through matched asymptotic expansions

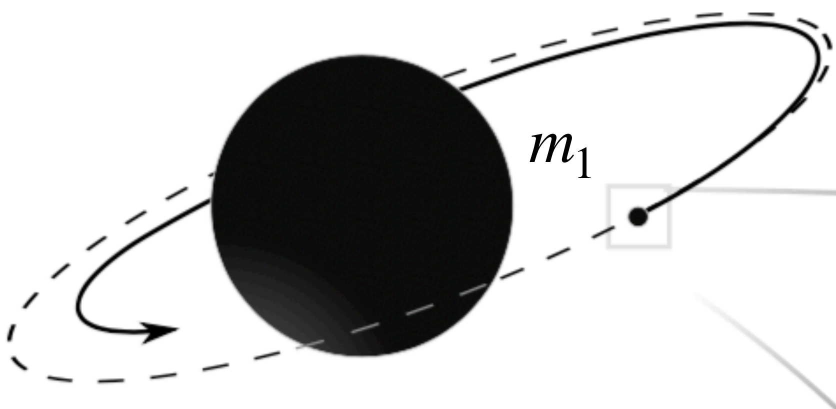

- outer expansion: treat field of m_1 as the background
- inner expansion: treat the field of m_2 as the background
- in buffer region: feed information from the inner to the outer expansion

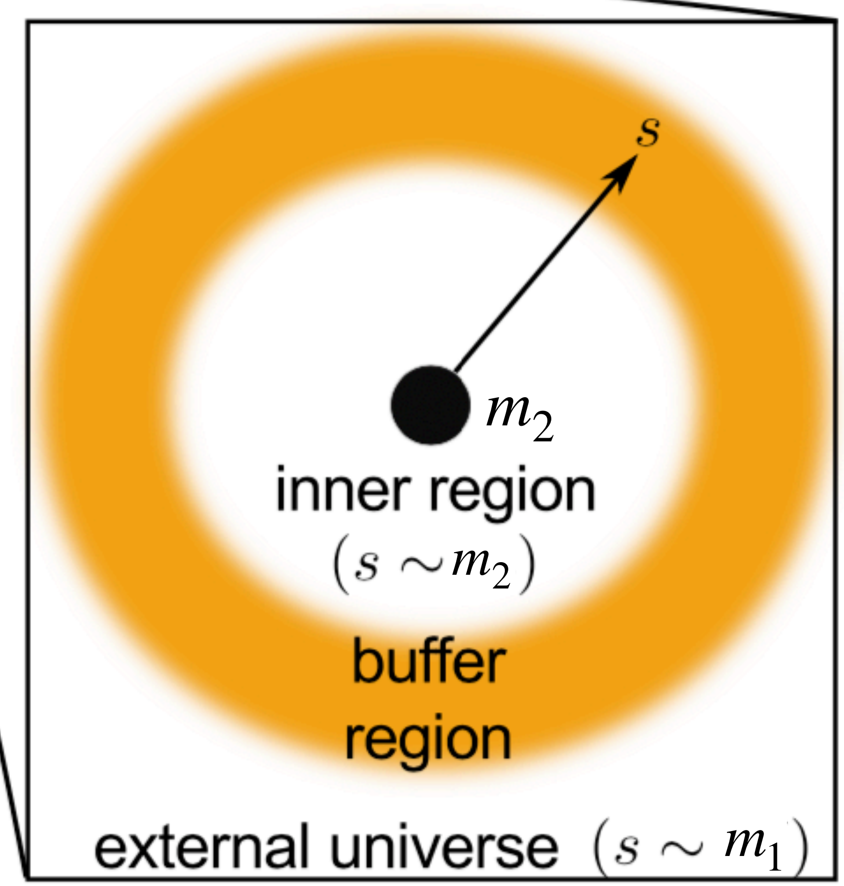

Image credit: A. Pound

For more details see: arXiv:gr-qc/9606018, arXiv:gr-qc/9610053, arXiv:1102.0529, arXiv:1201.5089, arXiv:1203.3189

Defining the self-force: regular/singular split

Through the matched expansion we can define (locally) a singular piece of the metric perturbation and a regular piece

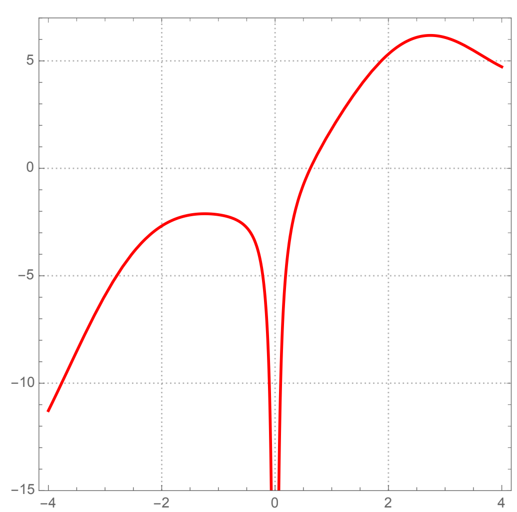

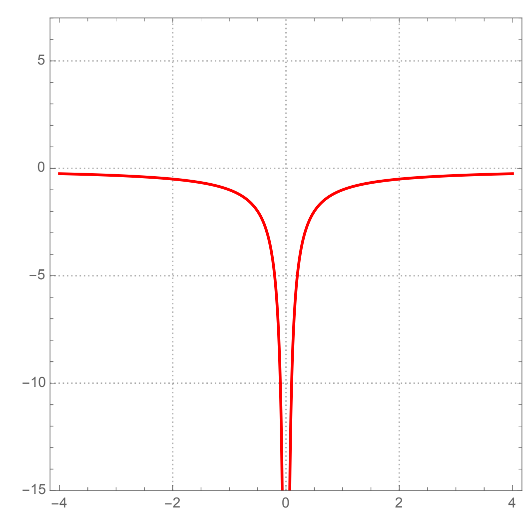

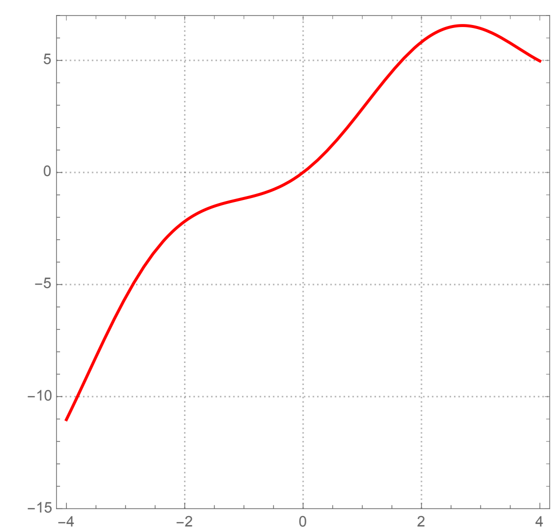

$$h^{ret} = h^{S} + h^{R}$$

The self-force depends on the derivative of the regular metric perturbation

$$F^{\alpha}_{self}[z_{\mu}(\tau)] = \lim_{x^{\mu} \to z^{\mu}(\tau)} F^{\alpha}[\nabla^{\alpha} h^{R}]$$

Rarely have the exact singular field, rather just a local approximation, which we call the puncture field h^{P}

Black Hole Perturbation Theory

A key question in any perturbative expansion is: how high in the expansion do I need to go in order to capture the physics I am interested in?

Waveform phase: $$\Phi(t) = \epsilon^{-1}\boxed{\Phi_{-1}(t)} + \epsilon^{0}\boxed{\Phi_{0}(t)} + \mathcal{O}(\epsilon)$$

Adiabatic

From the orbit averaged piece of first-order self-force $\langle F_1^\alpha \rangle$

$\langle F_1^\alpha \rangle$ can be related to the fluxes, thus avoiding a local calculation of the self-force

Good enough for detection and rough parameter estimation for astrophysics of EMRIs of bright sources

Post-Adiabatic order

Two contributions:

- Oscillatory pieces of the first order self-force
- Second-order orbit averaged self-force $\langle F_2^\alpha \rangle$

Needed to extract all sources

Needed for precision tests of GR

Potential application to IMRIs

Black Hole Perturbation Theory: field equations

$$G_{\alpha\beta}[\bar{g}_{\alpha\beta} + \epsilon h^{(1)}_{\alpha\beta} + \epsilon^2 h^{(2)}_{\alpha\beta}] = 8\pi T_{\alpha\beta}$$

Field equations from ϵ^n coefficients:

$$\epsilon^0 : \qquad G_{\alpha\beta}[\bar{g}] = 0$$

$$\epsilon^1 : \qquad \boxed{G^1_{\alpha\beta}}[h^1] = 8\pi T_{\alpha\beta}$$

$$\epsilon^2 : \qquad \boxed{G^1_{\alpha\beta}}[h^2] + G^2_{\alpha\beta}[h^1, h^1] = 0$$

Linearized Einstein operator

$$G^1_{\alpha\beta} = \partial_t^2 - \partial_{r*}^2 + \dots$$

$$\equiv \Box$$

Black Hole Perturbation Theory: field equations

$$G_{\alpha\beta}[\bar{g}_{\alpha\beta} + \epsilon h^{(1)}_{\alpha\beta} + \epsilon^2 h^{(2)}_{\alpha\beta}] = 8\pi T_{\alpha\beta}$$

Field equations from ϵ^n coefficients:

$$\epsilon^1 : \qquad \Box h^1 = 8\pi T$$

$$\epsilon^2 : \qquad \Box h^2 + G^2[h^1, h^1] = 0$$

Black Hole Perturbation Theory: field equations

$$G_{\alpha\beta}[\bar{g}_{\alpha\beta} + \epsilon h^{(1)}_{\alpha\beta} + \epsilon^2 h^{(2)}_{\alpha\beta}] = 8\pi T_{\alpha\beta}$$

Field equations from ϵ^n coefficients:

$$\epsilon^1 : \qquad \square h^1 = 8\pi T$$

$$\epsilon^2 : \qquad \square h^2 = -G^2[h^1, h^1]$$

Black Hole Perturbation Theory: field equations

$$G_{\alpha\beta}[\bar{g}_{\alpha\beta} + \epsilon h^{(1)}_{\alpha\beta} + \epsilon^2 h^{(2)}_{\alpha\beta}] = 8\pi T_{\alpha\beta}$$

Field equations from ϵ^n coefficients:

$$\epsilon^1 : \qquad \Box (h^{1R} + h^{1P}) = 8\pi T$$

$$\epsilon^2 : \qquad \Box (h^{2R} + h^{2P}) = -G^2[h^1, h^1]$$

Black Hole Perturbation Theory: field equations

$$G_{\alpha\beta}[\bar{g}_{\alpha\beta} + \epsilon h^{(1)}_{\alpha\beta} + \epsilon^2 h^{(2)}_{\alpha\beta}] = 8\pi T_{\alpha\beta}$$

Field equations from ϵ^n coefficients:

Usual point particle source

$$\epsilon^1 : \qquad \Box h^{1R} = 8\pi \boxed{T} - \Box h^{1P}$$

$$\epsilon^2 : \qquad \boxed{\Box} h^{2R} = - \boxed{G^2[h^1, h^1]} - \Box \boxed{h^{2P}}$$

$$\Box = \partial_t^2 - \partial_{r*}^2 + \ldots$$

- Non-compact
- Diverges at the particle

Crux:

- Pound (2012)*
- Gralla (2012)

Equations of motion take the form: $$\frac{D^2 z^\mu}{d\tau} = \epsilon F^{1\mu}[h^{R1}] + \epsilon^2 F^{2\mu}[h^{R2}]$$

Additional challenges:

- singular field known in Lorenz gauge $\nabla^\alpha \bar{h}_{\alpha\beta} = 0$
- but PDE Lorenz gauge field equations have never been stably evolved

*Pound, Phys. Rev. Lett. 109, 051101 (2012)

Many additional steps

- Move into frequency domain via a two-timescale expansion. We define a slow time $\tilde{t} = \epsilon t$ and fast time ϕ_p

$$\frac{\partial}{\partial t} = \frac{\partial \phi_p}{\partial t}\frac{\partial}{\partial \phi_p} + \frac{\partial \tilde{t}}{\partial t}\frac{\partial}{\partial \tilde{t}} = \Omega\frac{\partial}{\partial \phi_p} + \epsilon\frac{\partial}{\partial \tilde{t}} \implies \Box_\omega = \Box^0_\omega + \epsilon\,\Box^1_\omega$$

$$\boxed{\begin{aligned} \Box^0_\omega h^1 &= T^1 \\ \boxed{\Box^0_\omega} h^{R2} &= \boxed{G^2_\omega[h^1, h^1] - \Box^0_\omega h^{P2} - \Box^1_\omega h^1} \end{aligned}}$$

Effective-source

$$\Box^0_\omega = -\partial^2_{r*} - m^2\Omega^2_0 + \dots$$

- Effective-source in frequency domain methods
- Challenges on large length scales
- Challenges constructing $G^2_\omega[h^1, h^1]$
- For more details see recording of talk by Adam Pound at the Capra meeting for Radiation Reaction: https://www.youtube.com/watch?v=gQd2CsH4vug

For further details see: arXiv:1201.5089, arXiv:1206.6538, arXiv:1311.3104, arXiv:1404.1543, arXiv:1505.07841, arXiv:1510.05172, arXiv:1608.06783, arXiv:1703.02836, arXiv:1908.07419, arXiv:2006.11263

Results at first-order in the mass-ratio

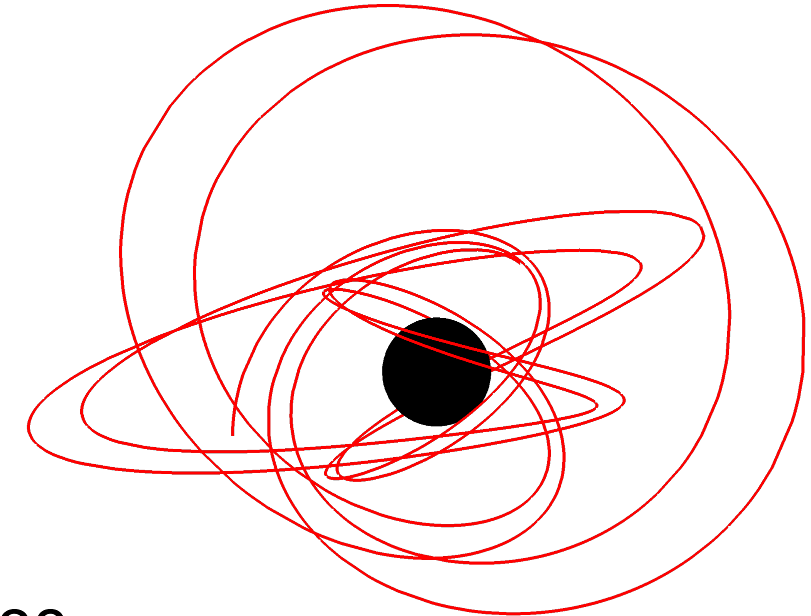

$$\epsilon^1 : \qquad \Box h^{1R} = 8\pi T - \Box h^{1P}$$

- We have known how to compute h^{1P} since 1997. It took ~20 years to compute the h^{1R} for generic motion about a Kerr black hole [van de Meet, arXiv:1711.09607]

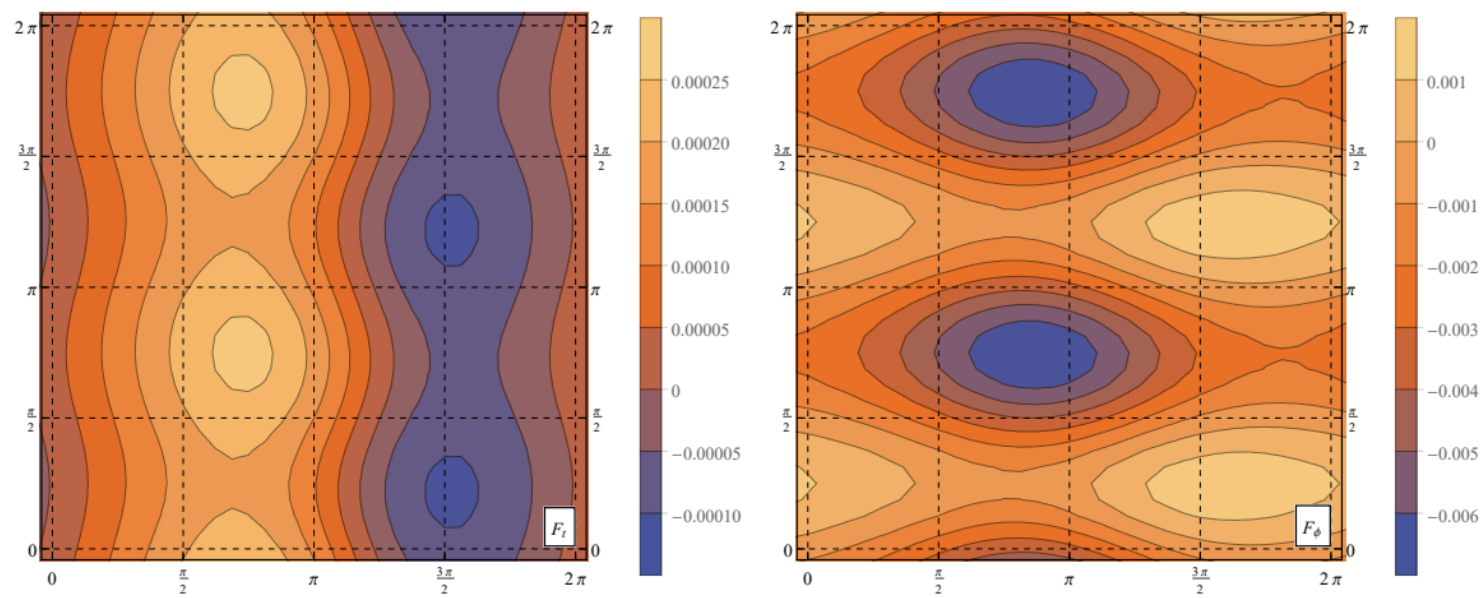

- We have just started to explore the situation when the secondary is spinning (more on this later) [arXiv:1912.09461, 2004.02654]

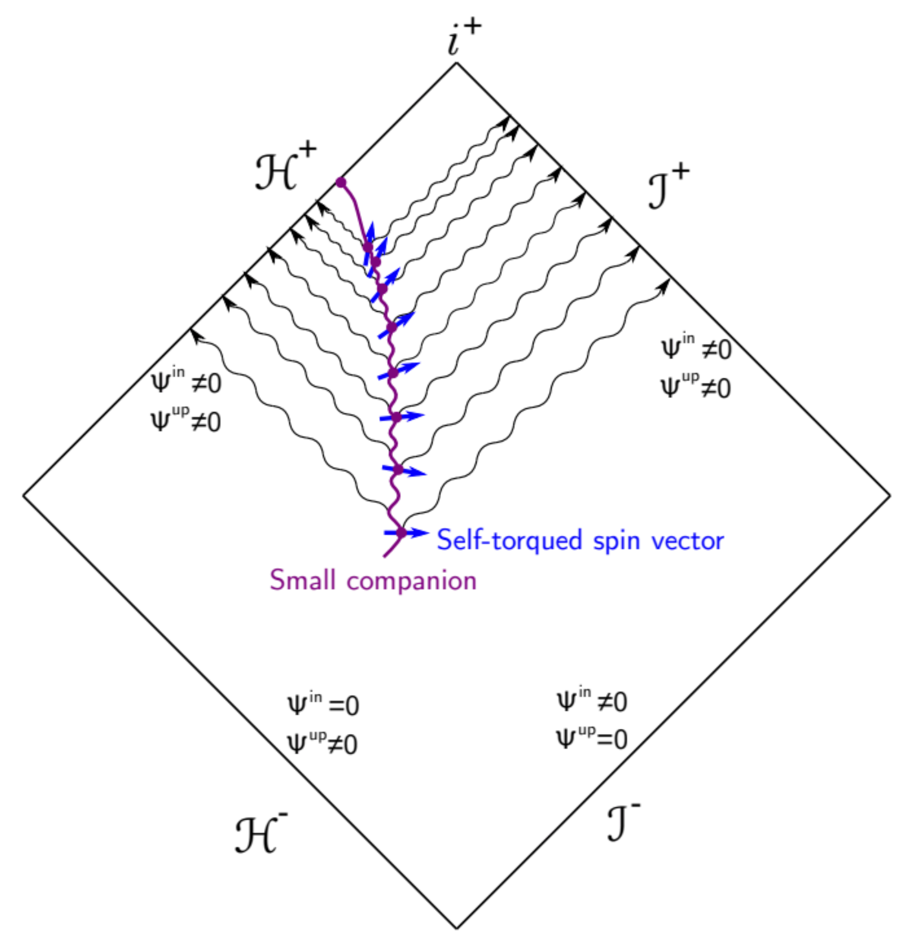

Results at first-order in the mass-ratio

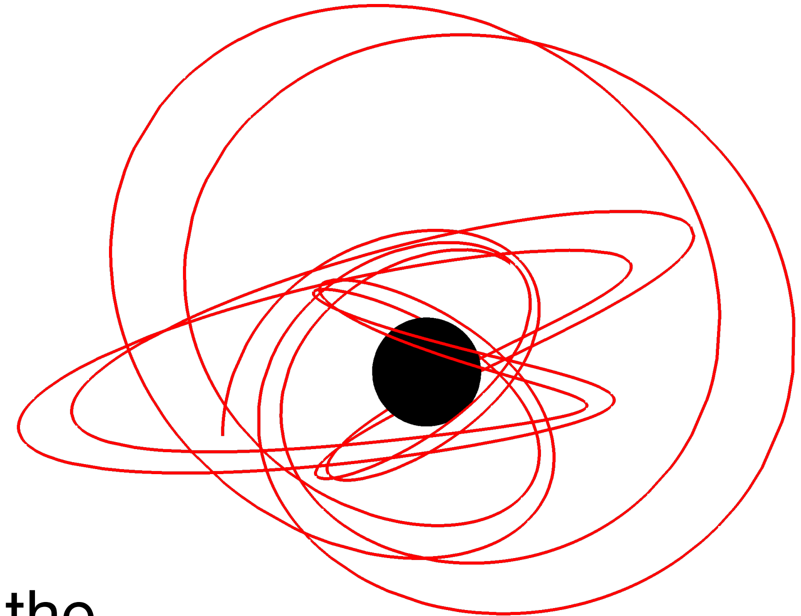

$$\epsilon^1 : \qquad \Box h^{1R} = 8\pi T - \Box h^{1P}$$

- We can also solve the equations of motion and compute the inspiral trajectory and the associated waveform

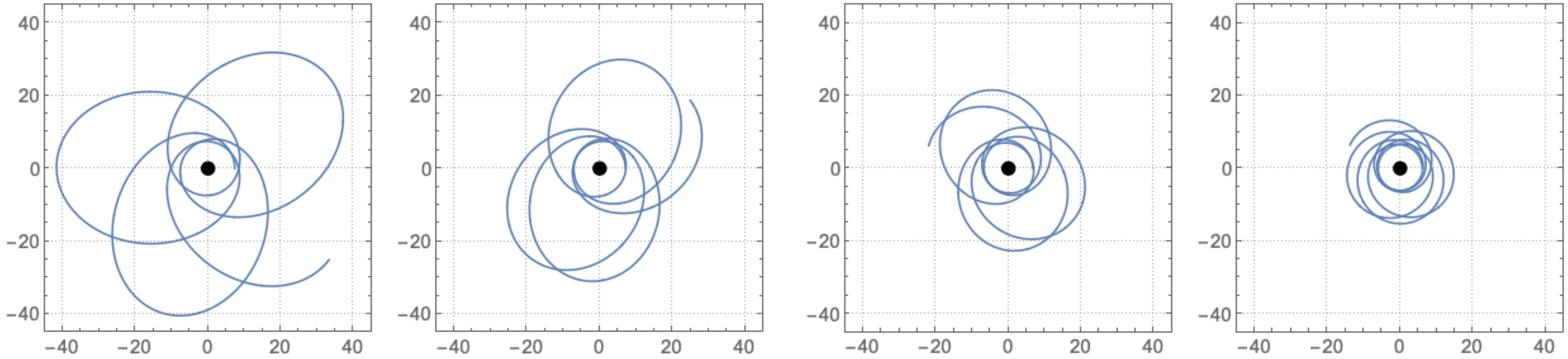

- Recent work has shown how to compute waveforms with 100's of thousands of cycles in milliseconds using neutral network and GPU techniques [arXiv:2008.06071]

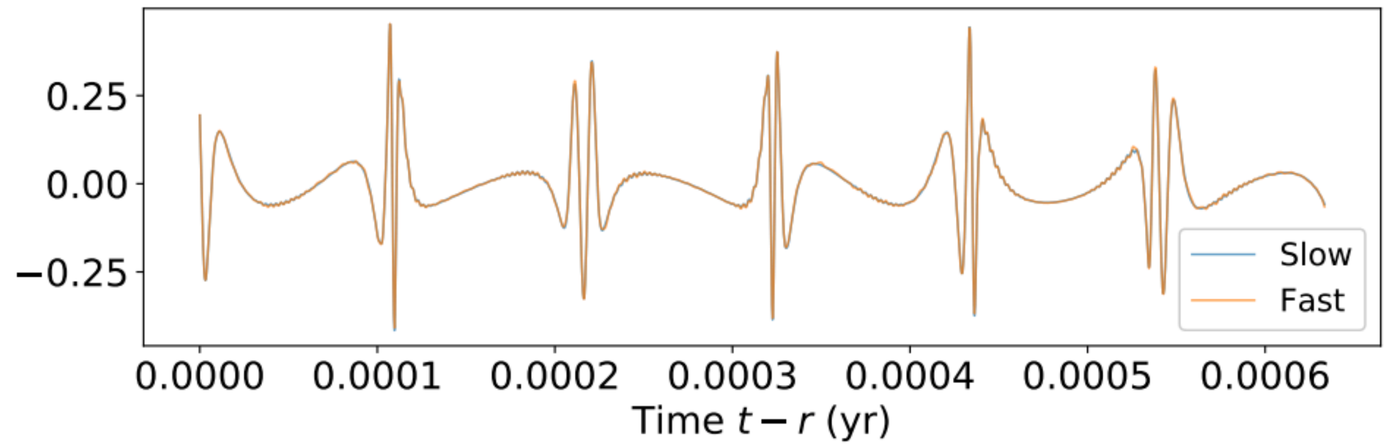

New results at second-order in the mass-ratio

The remainder of this talk will focus on brand new (unpublished) results from calculations at second-order in the mass-ratio

$$\epsilon^1: \qquad \Box h^{1R} = 8\pi T - \Box h^{1P}$$

$$\epsilon^2: \qquad \Box h^{2R} = -G^2[h^1, h^1] - \Box h^{2P}$$

- The main challenge is computing the source to the second-order equation

- We will start with the simplest binary configuration: quasi-circular inspirals into a Schwarzschild black hole

- Within the two-timescale framework we can solve the above field equation and compute the GW flux $\mathscr{F}(r_0)$

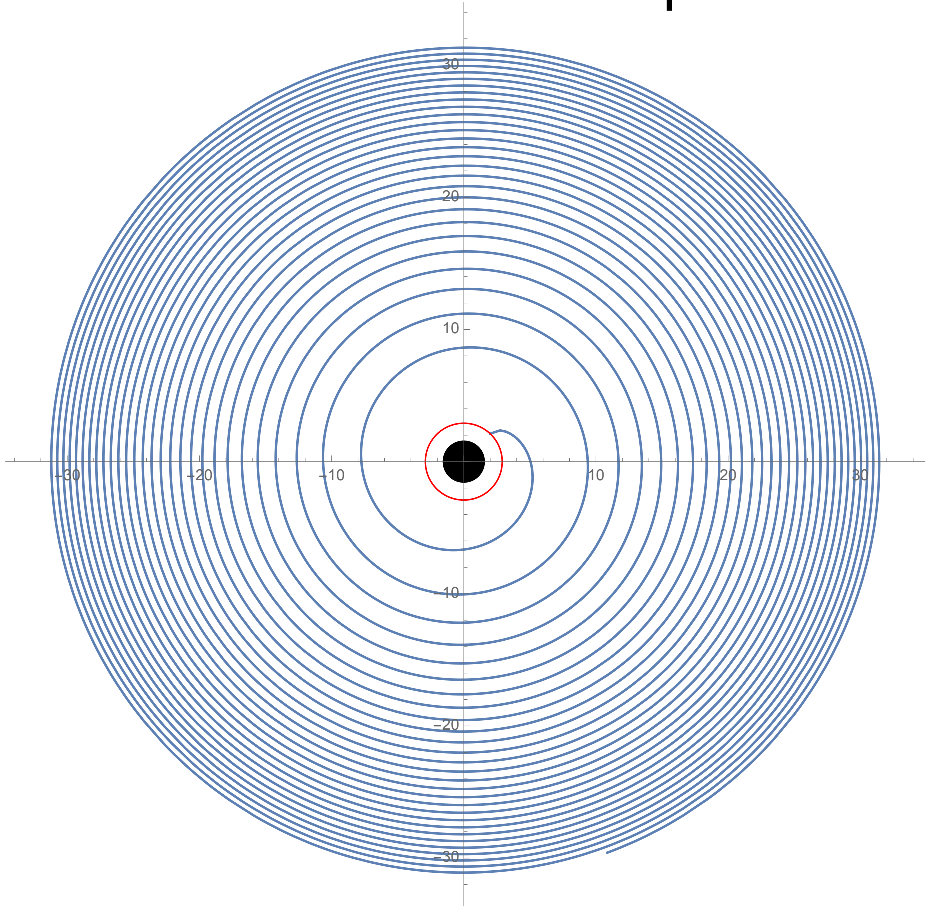

Expansion in the symmetric mass ratio

So far we have been expanding using the small mass-ratio $\epsilon = m_2/m_1$

Let's also introduce the large mass-ratio $q = m_1/m_2 = 1/\epsilon$ and the symmetric mass-ratio:

$$\nu = \frac{m_1 m_2}{M^2} = \frac{q}{(1+q)^2}$$

where $M = m_1 + m_2$

Also instead of parametrising the orbit by r_0 we will use $x = (M\Omega)^{2/3}$

Using these definitions we can rewrite

$$\mathcal{F}(r_0, \epsilon) = \epsilon^2 \mathcal{F}^{(1)}(r_0) + \epsilon^3 \mathcal{F}^{(2)}(r_0) + O(\epsilon^4)$$

the form

$$\mathcal{F}(x, \nu) = \nu^2 \mathcal{F}_\nu^{(1)}(x) + \nu^3 \mathcal{F}_\nu^{(2)}(x) + O(\nu^4)$$

where $\mathcal{F}_\nu^{(1)} = \mathcal{F}^{(1)}, \quad \mathcal{F}_\nu^{(2)} = \mathcal{F}_\nu^{(2)}(\mathcal{F}^{(1)}, \mathcal{F}^{(2)}, d\mathcal{F}^{(1)}/dx)$

Comparison with post-Newtonian theory

For this talk, let's look at the $l = 3, m = 1$ mode

The (3,3) and (3,1) fluxes were derived to 3.5 PN order in Faye+ arXiv:1409.3546

$$\mathcal{F}_{31}^{PN} = \left(\frac{\nu^2}{1260} - \frac{\nu^3}{315}\right)x^6 + \left(-\frac{4\nu^2}{945} + \frac{\nu^3}{63} + \frac{4\nu^4}{945}\right)x^7 + \left(\frac{\pi\nu^2}{630} - \frac{2\pi\nu^3}{315}\right)x^{15/2} + O(x^8)$$

We want to compare agains the $O(\nu^3)$ pieces of this

$$\mathcal{F}_{31}^{(2)PN} = -\frac{x^6}{315} + \frac{x^7}{63} - \frac{2}{315}\pi x^{15/2} - \frac{1291x^8}{31185} + \frac{13}{420}\pi x^{17/2}$$
$$+x^9\left(\frac{26\log(x)}{6615} - \frac{389\pi^2}{120960} + \frac{52\gamma}{6615} - \frac{117030737}{7945938000} - \frac{\log^2(1024)}{7875} + \frac{4\log^2(2)}{315} + \frac{52\log(2)}{6615}\right) + O(x^{19/2})$$

This is all the known terms at $O(\nu^3)$ for the (3,1) mode up to 3.5PN

Comparison with post-Newtonian theory

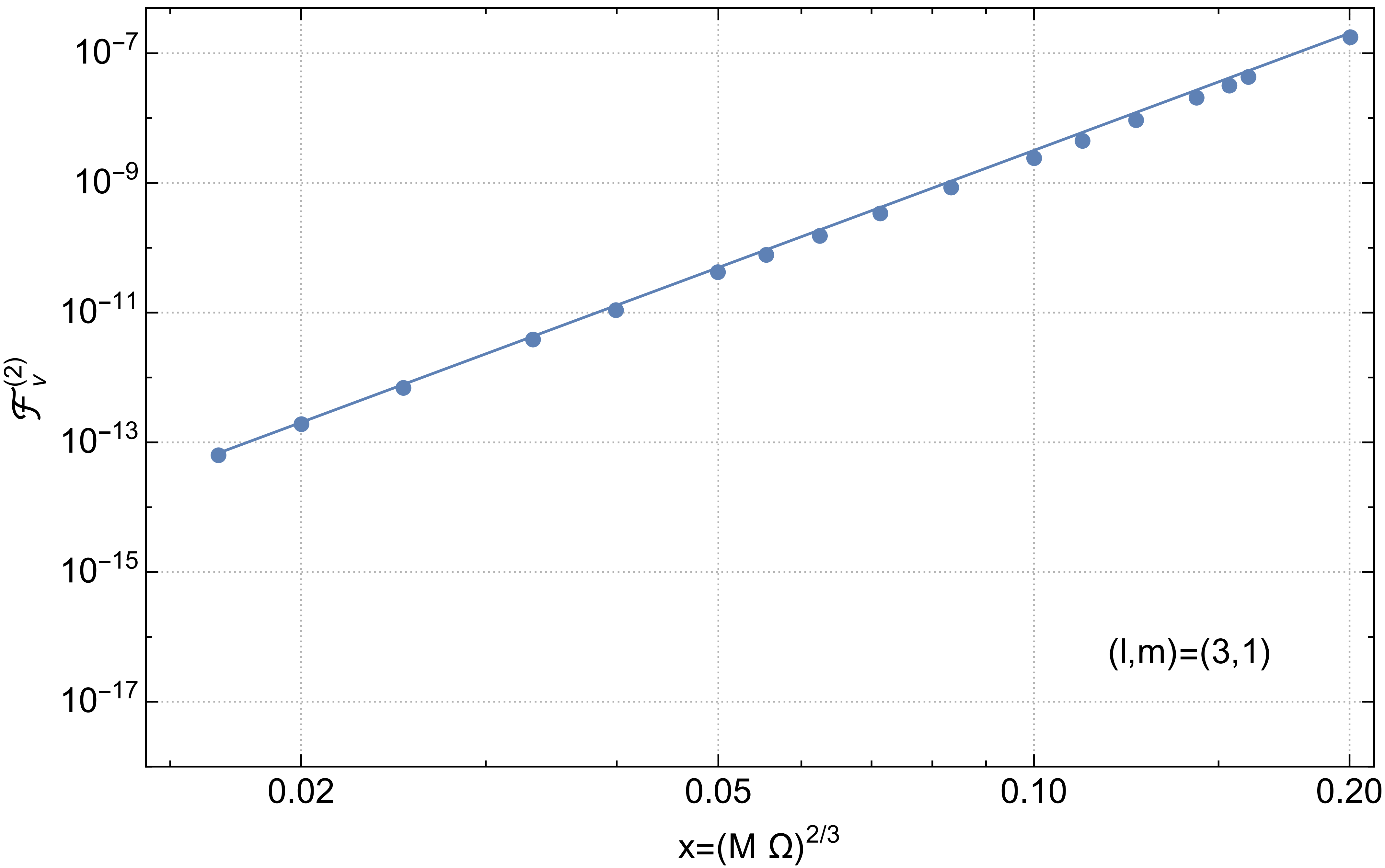

$$\mathcal{F}_{31}^{(2)PN} = \boxed{-\frac{x^6}{315}} + \frac{x^7}{63} - \frac{2}{315}\pi x^{15/2} - \frac{1291 x^8}{31185} + \frac{13}{420}\pi x^{17/2}$$
$$+ x^9 \left(\frac{26\log(x)}{6615} - \frac{389\pi^2}{120960} + \frac{52\gamma}{6615} - \frac{117030737}{7945938000} - \frac{\log^2(1024)}{7875} + \frac{4\log^2(2)}{315} + \frac{52\log(2)}{6615} \right) + O(x^{19/2})$$

Comparison with post-Newtonian theory

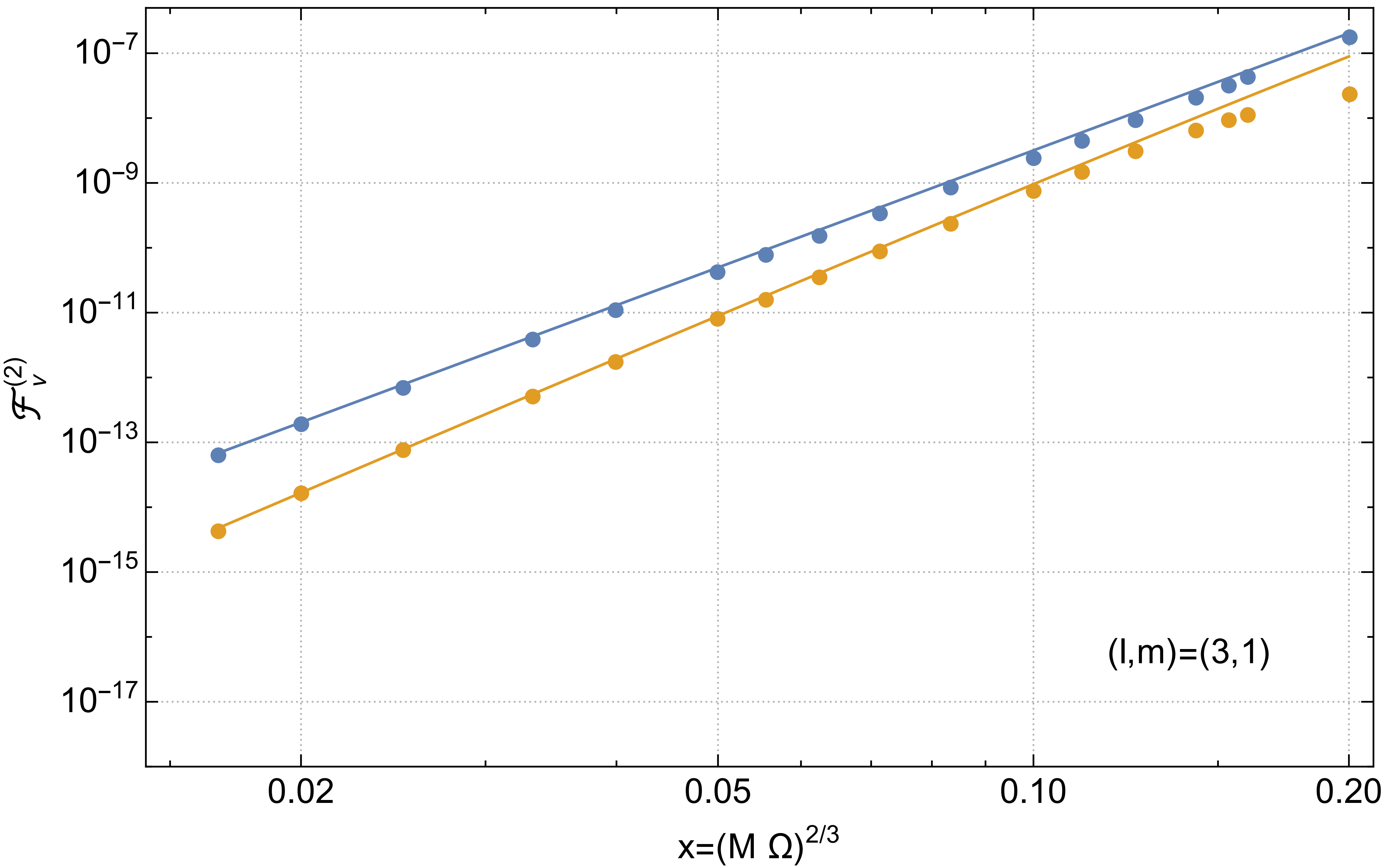

$$\mathcal{F}^{(2)PN}_{31} = \boxed{-\frac{x^6}{315}} \boxed{+\frac{x^7}{63} - \frac{2}{315}\pi x^{15/2}} - \frac{1291x^8}{31185} + \frac{13}{420}\pi x^{17/2}$$

$$+x^9\left(\frac{26\log(x)}{6615} - \frac{389\pi^2}{120960} + \frac{52\gamma}{6615} - \frac{117030737}{7945938000} - \frac{\log^2(1024)}{7875} + \frac{4\log^2(2)}{315} + \frac{52\log(2)}{6615}\right) + O(x^{19/2})$$

Comparison with post-Newtonian theory

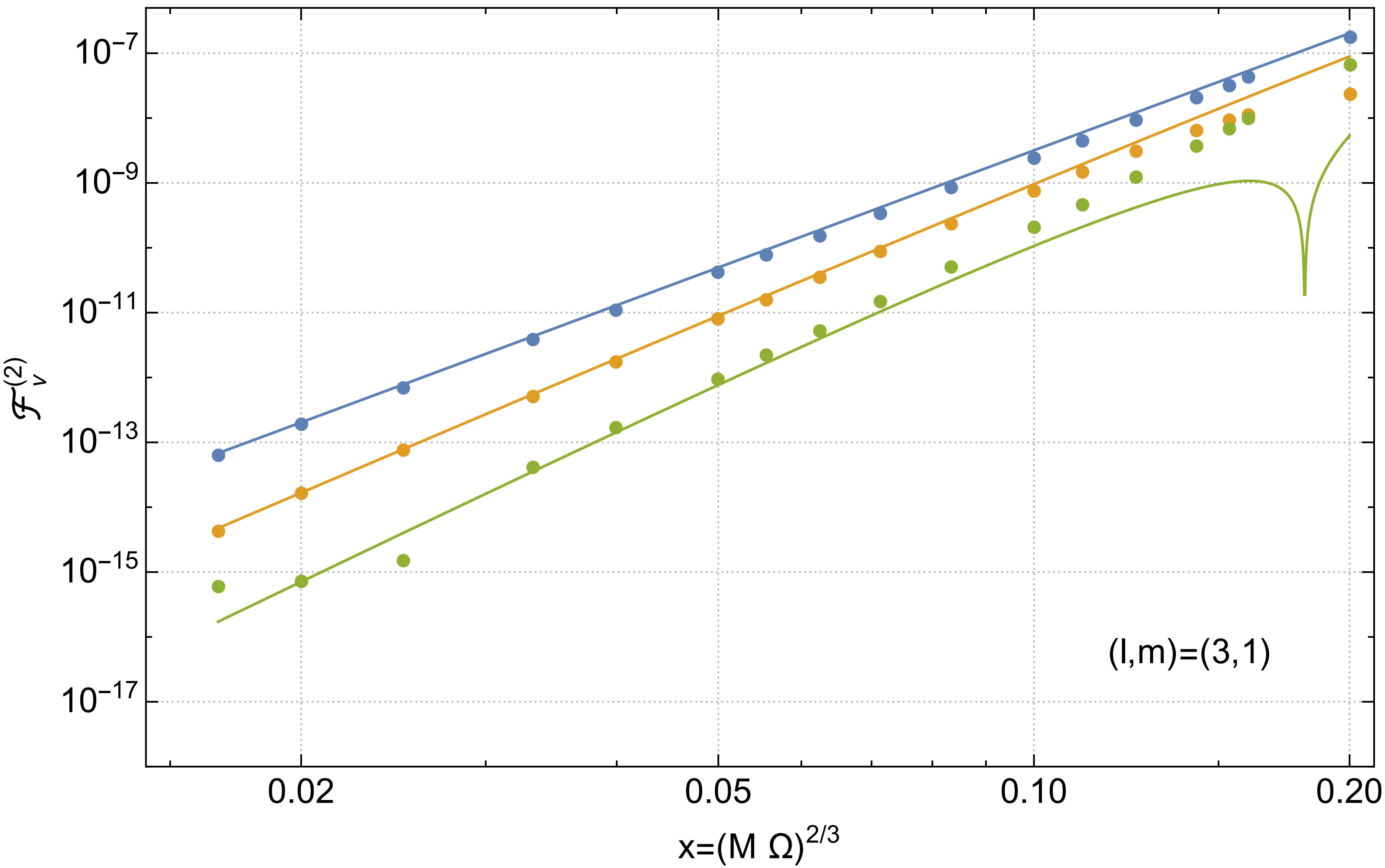

$$\mathscr{F}^{(2)PN}_{31} = \boxed{-\frac{x^6}{315}} \boxed{+\frac{x^7}{63} - \frac{2}{315}\pi x^{15/2}} \boxed{-\frac{1291 x^8}{31185} + \frac{13}{420}\pi x^{17/2}}$$

$$+x^9\left(\frac{26\log(x)}{6615} - \frac{389\pi^2}{120960} + \frac{52\gamma}{6615} - \frac{117030737}{7945938000} - \frac{\log^2(1024)}{7875} + \frac{4\log^2(2)}{315} + \frac{52\log(2)}{6615}\right) + O(x^{19/2})$$

Comparison with post-Newtonian theory

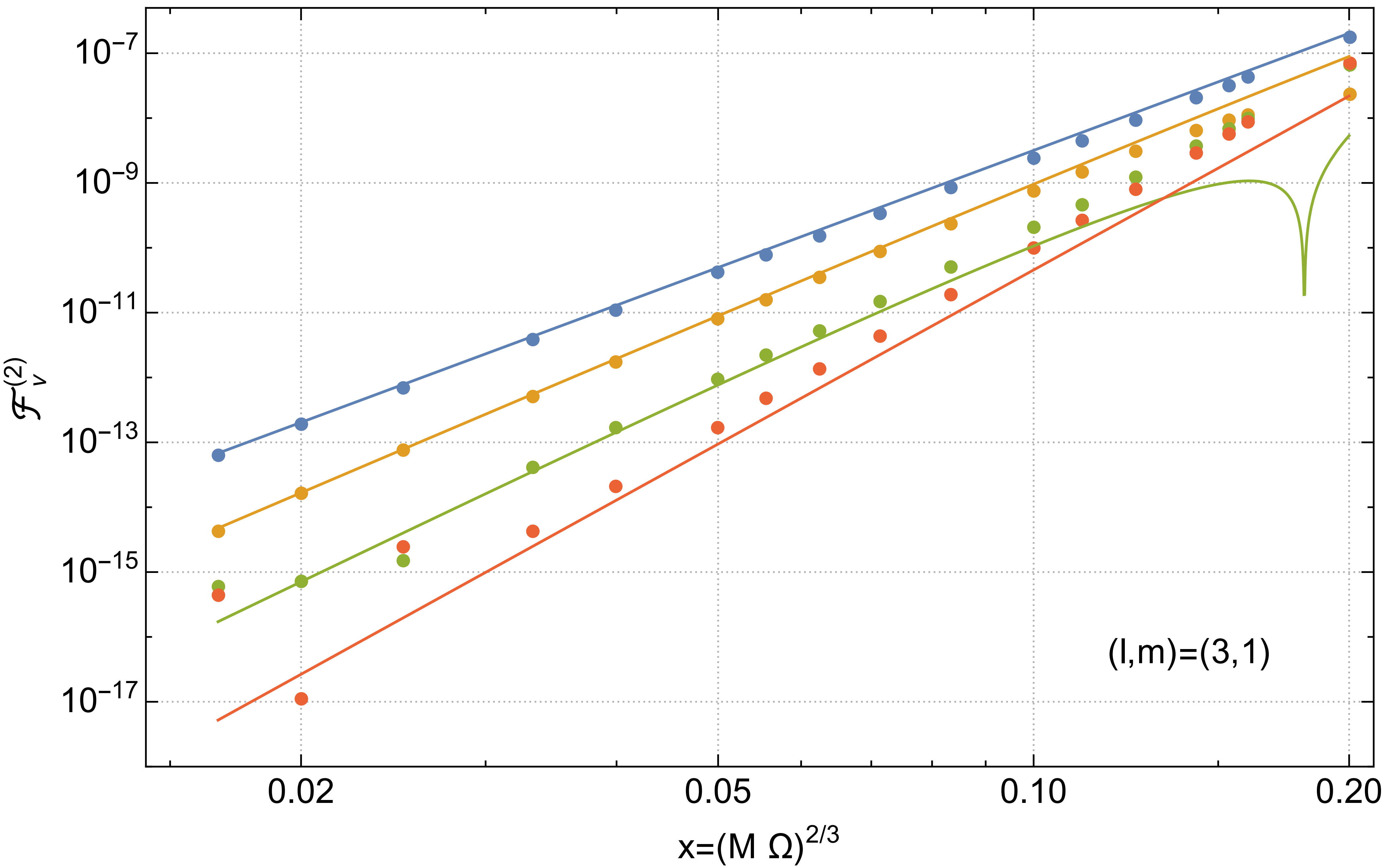

$$\mathcal{F}_{31}^{(2)PN} = \boxed{-\frac{x^6}{315}} \boxed{+\frac{x^7}{63} - \frac{2}{315}\pi x^{15/2}} \boxed{-\frac{1291 x^8}{31185} + \frac{13}{420}\pi x^{17/2}}$$
$$\boxed{+x^9\left(\frac{26\log(x)}{6615} - \frac{389\pi^2}{120960} + \frac{52\gamma}{6615} - \frac{117030737}{7945938000} - \frac{\log^2(1024)}{7875} + \frac{4\log^2(2)}{315} + \frac{52\log(2)}{6615}\right)} + O(x^{19/2})$$

Comparison with post-Newtonian theory

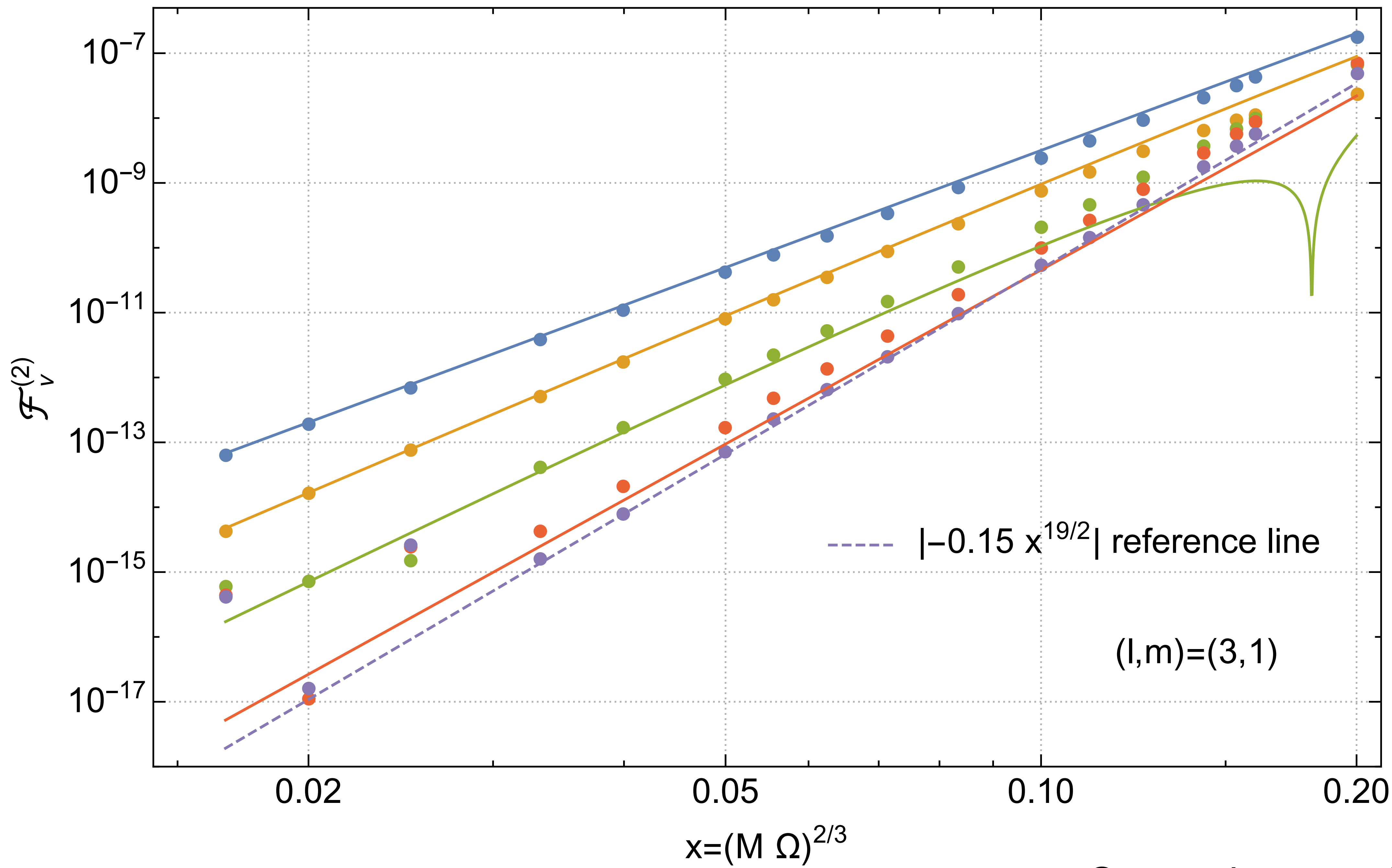

$$\mathcal{F}_{31}^{(2)PN} = \boxed{-\frac{x^6}{315}} \boxed{+\frac{x^7}{63} - \frac{2}{315}\pi x^{15/2}} \boxed{-\frac{1291x^8}{31185} + \frac{13}{420}\pi x^{17/2}}$$
$$\boxed{+x^9\left(\frac{26\log(x)}{6615} - \frac{389\pi^2}{120960} + \frac{52\gamma}{6615} - \frac{117030737}{7945938000} - \frac{\log^2(1024)}{7875} + \frac{4\log^2(2)}{315} + \frac{52\log(2)}{6615}\right)} + O(x^{19/2})$$

Can estimate unknown $O(\nu^3)$ PN terms

Comparison with numerical relativity

For this comparison it's useful to consider the flux normalised by the leading PN coefficient, e.g., for the (2,2) PN flux we have

$$\mathcal{F}_{22}^{PN} = \frac{32\nu^2 x^5}{5} + \frac{32}{105}\nu^2(55\nu - 107)x^6 + \frac{128}{5}\pi\nu^2 x^{13/2} + O\left(x^7\right)$$

$$\hat{\mathcal{F}}_{22}^{PN} = \frac{\mathcal{F}_{22}^{PN}}{\mathcal{F}_{22}^{0PN}} = 1 + \frac{1}{21}(55\nu - 107)x + 4\pi x^{3/2} + O\left(x^2\right)$$

To compute the NR flux we write the waveform as $h_{lm}(t) = A_{lm}(t)e^{i\Phi_{lm}(t)}$

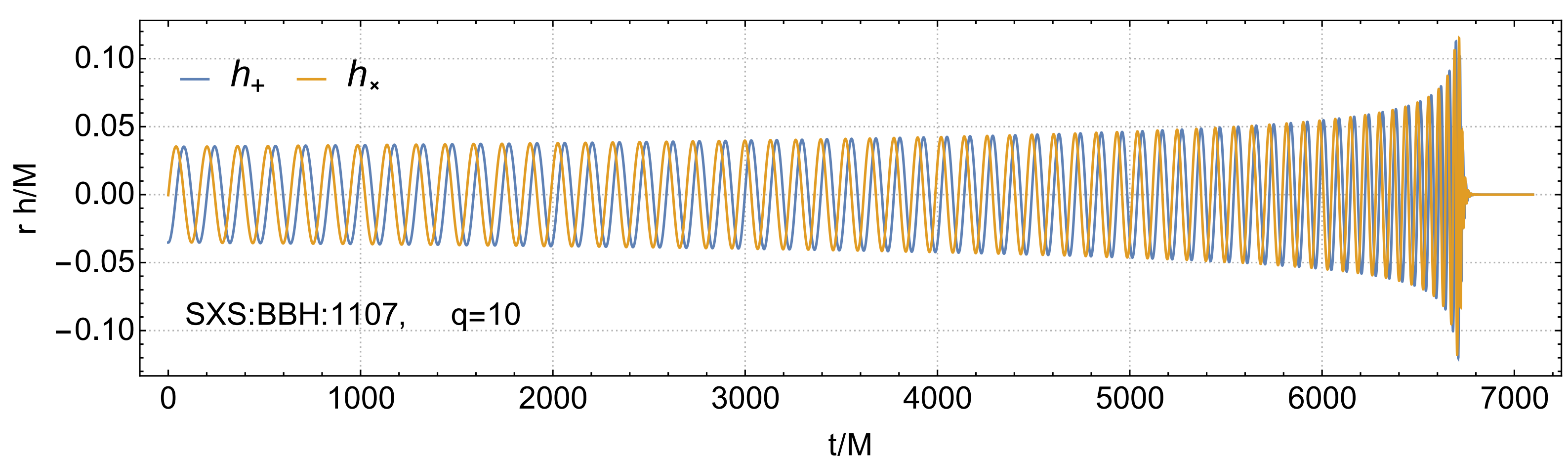

$$\mathcal{F}_{lm}^{NR}(t) = \frac{1}{16\pi}|\dot{h}_{lm}(t)|^2 \qquad x(t) = (M\dot{\Phi}(t)/m)^{2/3}$$

From these two we can compute $\mathcal{F}_{lm}^{NR}(x)$

Comparison with numerical relativity

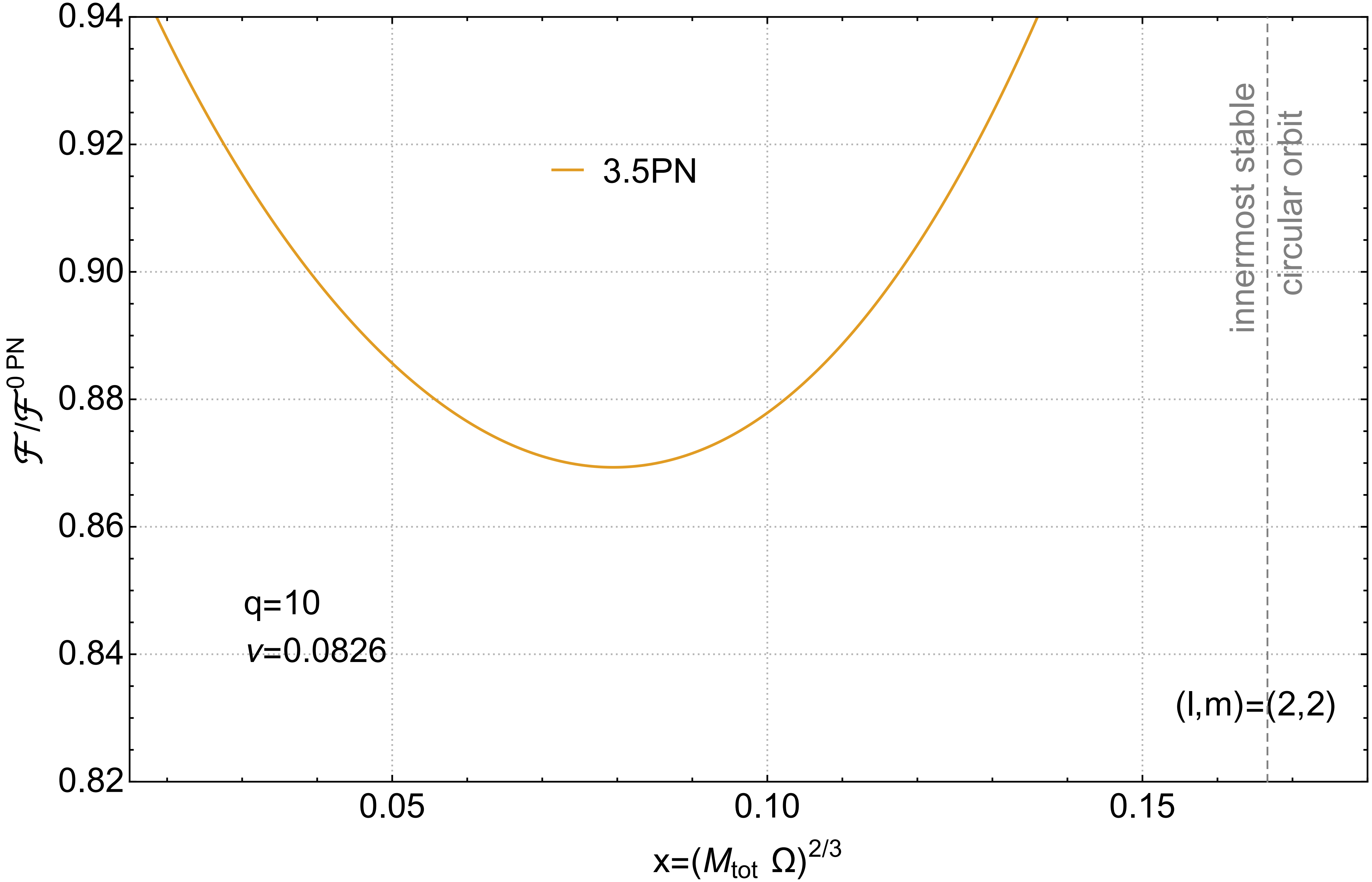

3.5PN series from Faye+ arXiv:1204.1043

Comparison with numerical relativity

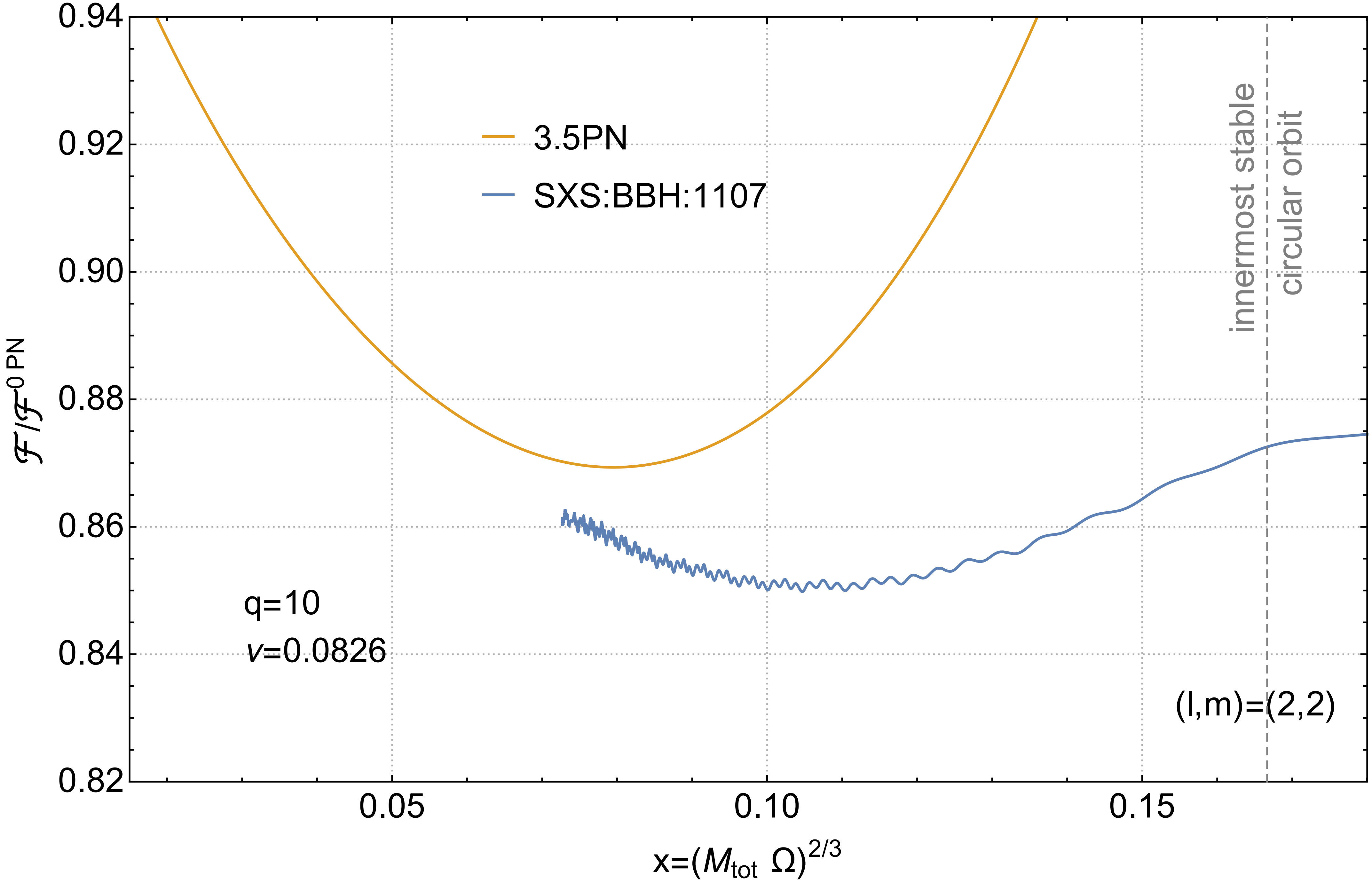

3.5PN series from Faye+ arXiv:1204.1043

NR data from SXS:BBH:1132

Comparison with numerical relativity

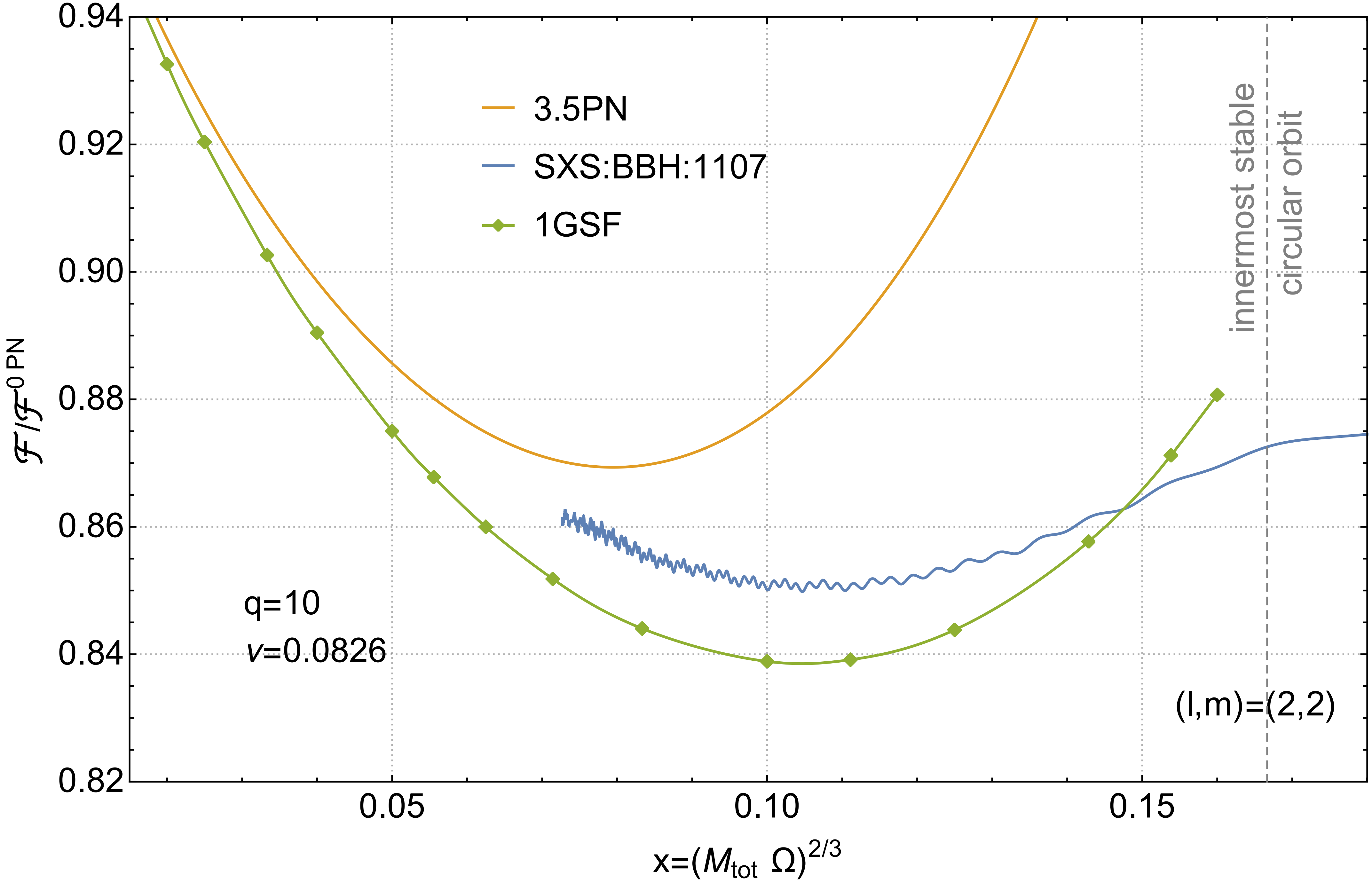

3.5PN series from Faye+ arXiv:1204.1043

NR data from SXS:BBH:1132

Comparison with numerical relativity

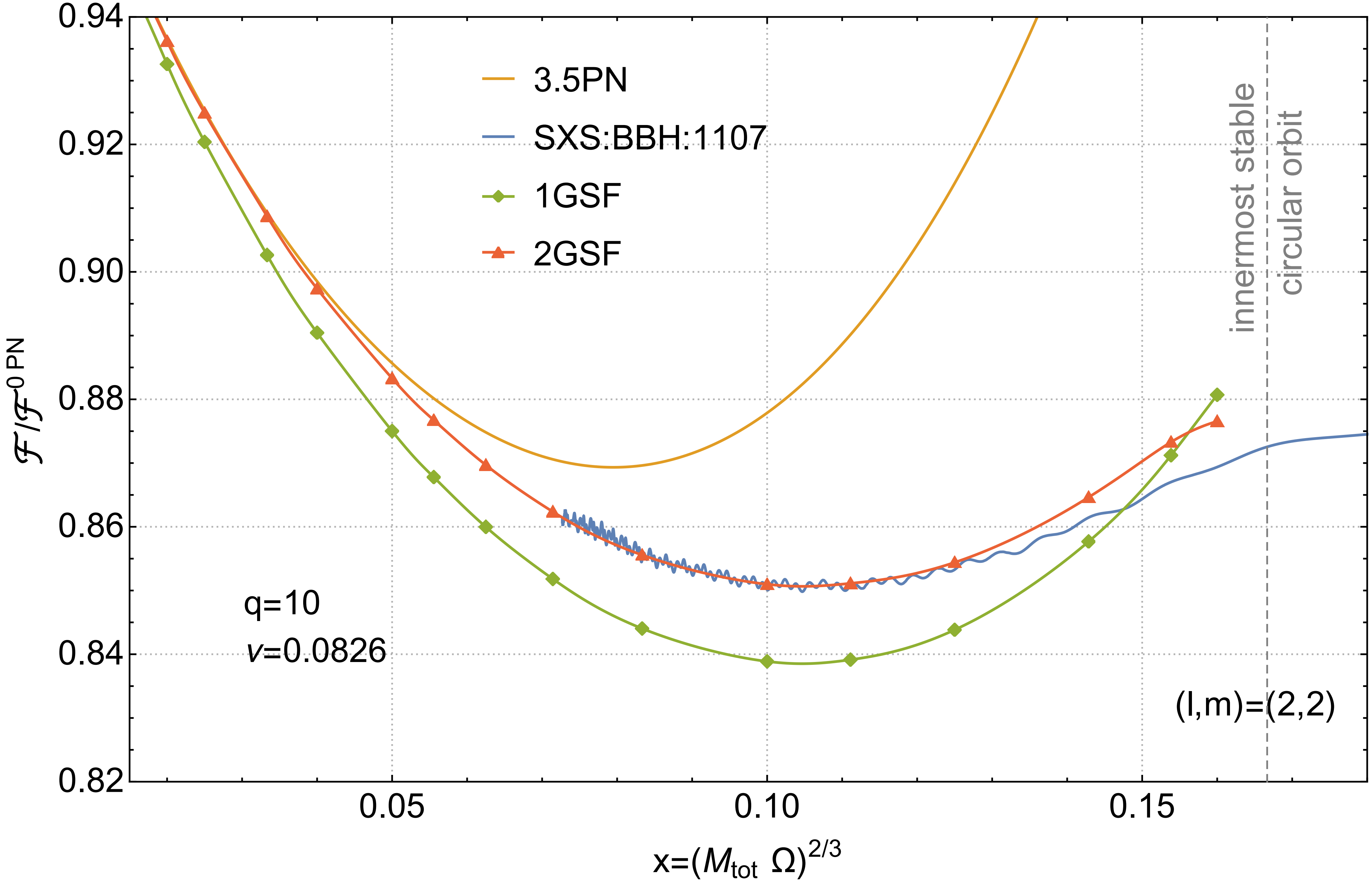

3.5PN series from Faye+ arXiv:1204.1043

NR data from SXS:BBH:1132

2GSF result by NW, B. Wardell, A. Pound and J. Miller (2020 in prep)

Comparison with numerical relativity

Equal mass binaries: $q = 1,\ \nu = 1/4$

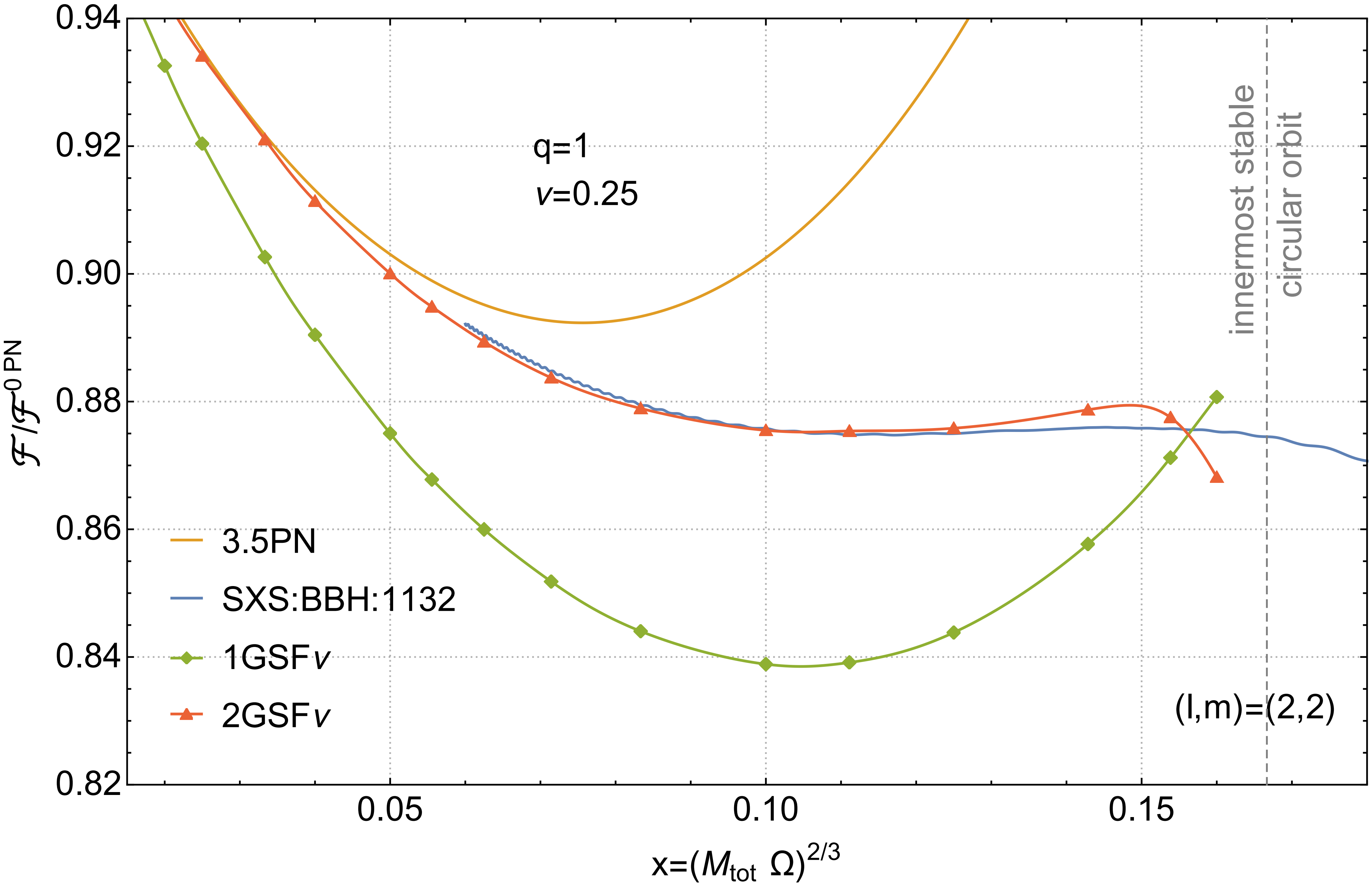

3.5PN series from Faye+ arXiv:1204.1043

NR data from SXS:BBH:1132

2GSF result by NW, B. Wardell, A. Pound and J. Miller (2020 in prep)

Comparison with numerical relativity

Higher modes

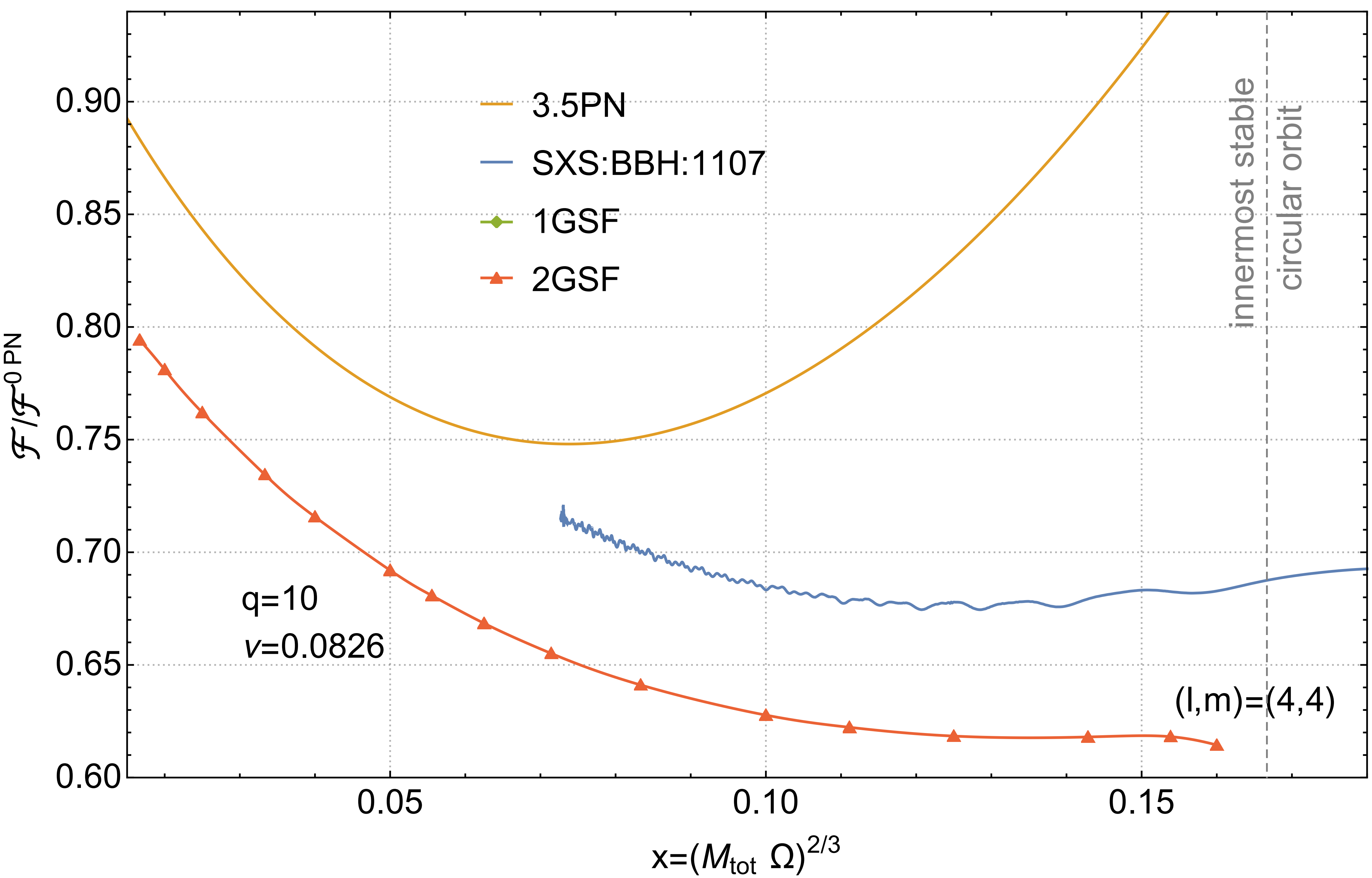

Comparison with numerical relativity

Higher modes

Why does the second-order flux not compare well against NR for the (4,4)-mode?

$$\mathcal{F}_{44}^{PN,leading} = \frac{8192}{567}\left(\nu^2 - 6\nu^3 + 9\nu^4\right)x^7$$

Compare this with the PN series for the (2,2)-mode:

$$\mathcal{F}_{22}^{PN} = \frac{32\nu^2 x^5}{5} + \frac{32}{105}\nu^2(55\nu - 107)x^6 + \frac{128}{5}\pi\nu^2 x^{13/2} + \frac{8\left(19136\nu^2 - 87691\nu^3 + 23404\nu^4\right)x^7}{6615} + O\left(x^{15/2}\right)$$

We can try a simple resummation to include some $\nu^{n\geq 4}$ information from the PN series

$$\mathcal{F}_{44}^{2GSF,resum} = \left[\frac{\nu^2\mathcal{F}_{44}^{1GSF\nu} + \nu^3\mathcal{F}_{44}^{2GSF\nu}}{\mathcal{F}_{44}^{PN,leading}} + O(\nu^4)\right]\mathcal{F}_{44}^{PN,leading}$$

This ensures that $\hat{\mathcal{F}}_{44}^{2GSF,resum} = 1 + \ldots$

Comparison with numerical relativity

Higher modes

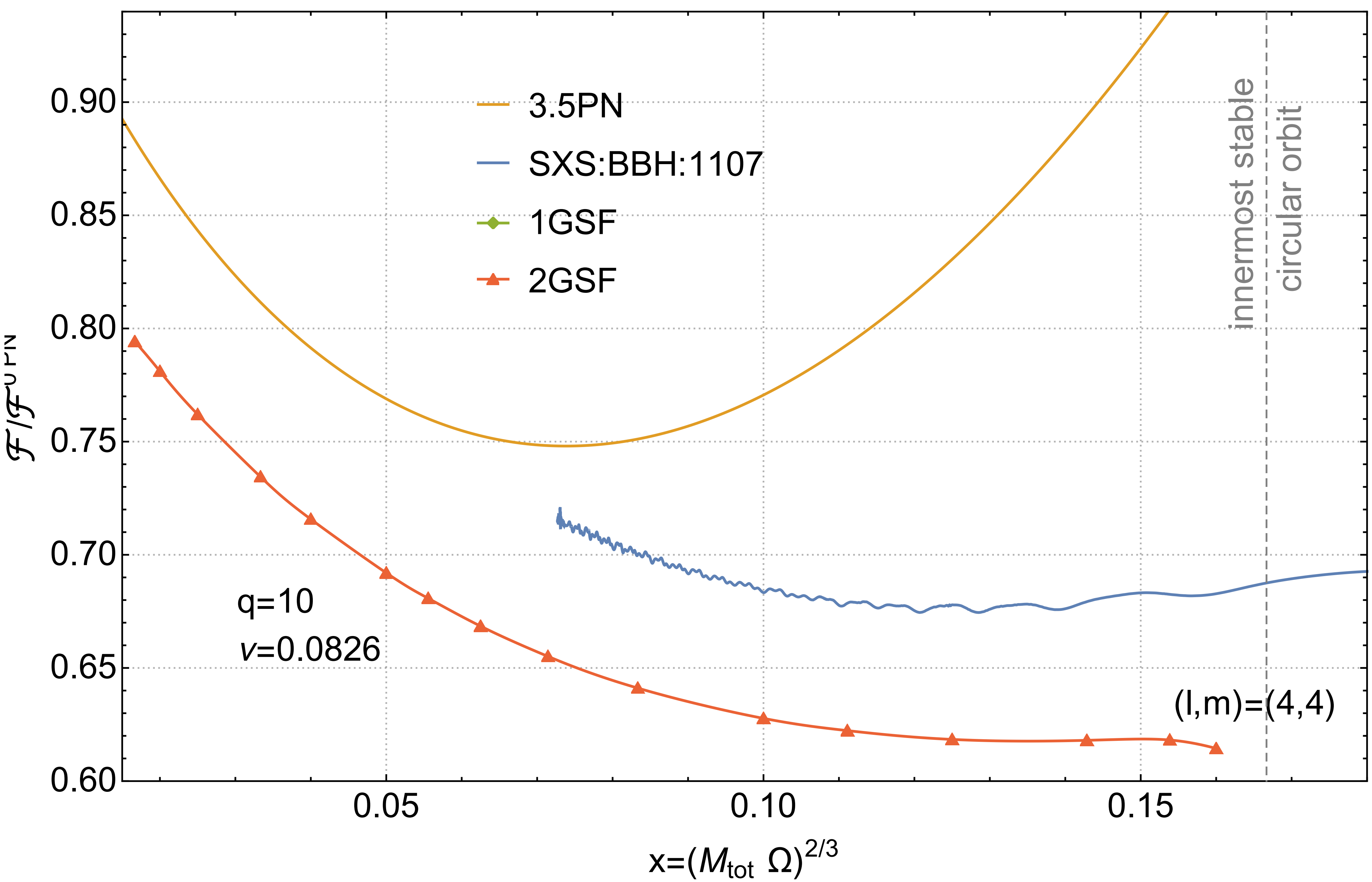

Comparison with numerical relativity

Higher modes

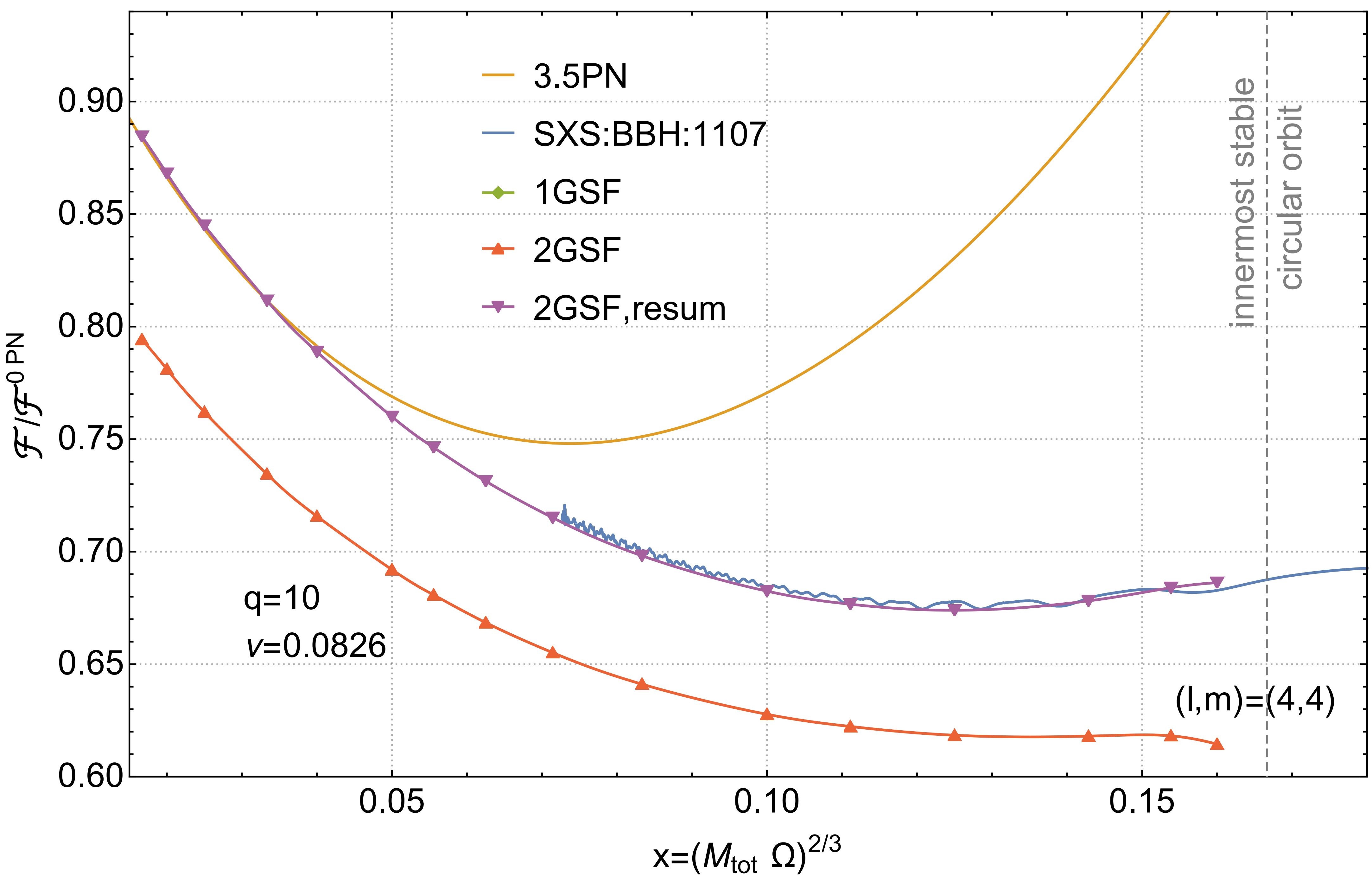

Comparison with numerical relativity

Higher modes

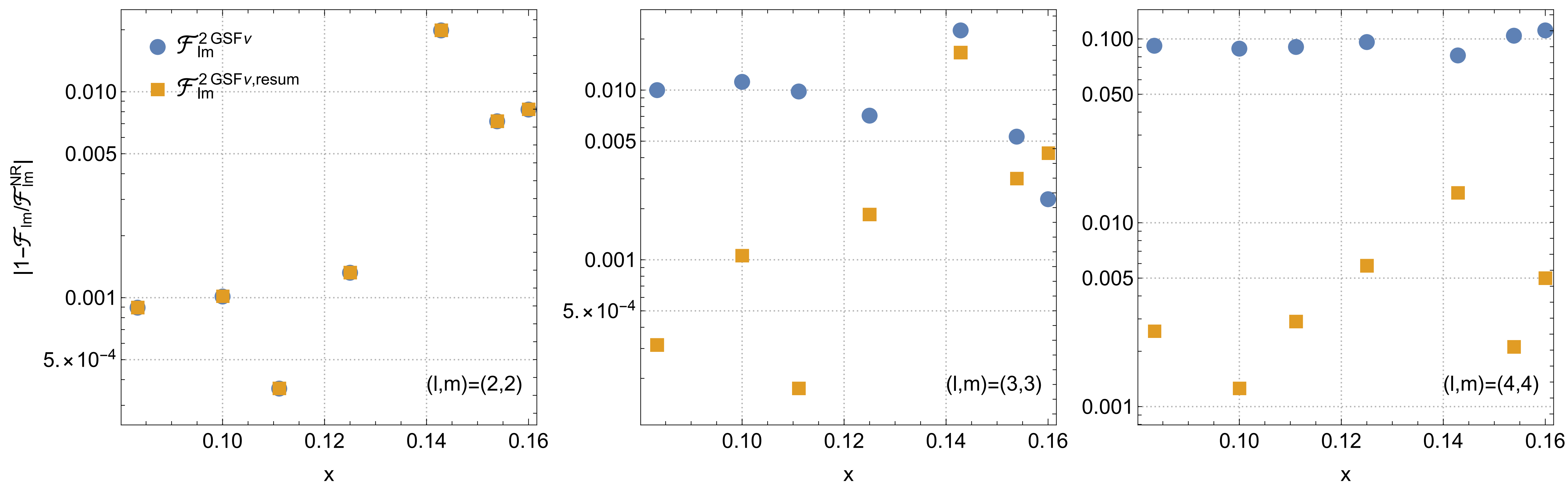

Pure 2GSF comparison with NR worsens for higher (l, m)-modes

- suggests that 2GSF comparison will be worse for orbits with lots of power in higher modes, e.g., highly eccentric or strong-field Kerr orbits

But… higher modes contribute less to the total flux and it seems a simple resummation can give large improvements

Spinning secondary results

For the second-order calculation, when we expanded the metric of the binary we did so about a Schwarzschild primary

$$g_{\alpha\beta} = \bar{g}_{\alpha\beta} + \epsilon h^{(1)}_{\alpha\beta} + \epsilon^2 h^{(2)}_{\alpha\beta} + \mathcal{O}(\epsilon^3)$$

Schwarzschild or Kerr

To model a spinning primary will be a lot more work. One major reason for this is that we need to change gauge as the Lorenz gauge is not separable in Kerr spacetime.

But we can model the spin on the secondary within the pole-dipole approximation

$$\epsilon = m_2/m_1, \qquad \sigma \equiv S_2/(m_1 m_2)$$

For self-force calculations the most relevant case is $\epsilon \sim \sigma$, which describes a compact secondary such as a black hole or neutron star

$$g_{\alpha\beta} = \bar{g}_{\alpha\beta} + \epsilon h^{(1)}_{\alpha\beta} + \sigma\epsilon h^{(1\sigma)}_{\alpha\beta} + \epsilon^2 h^{(2)}_{\alpha\beta} + \mathcal{O}(\epsilon^3)$$

Spinning secondary results

Also expand the stress energy tensor
$T_{\alpha\beta} = \epsilon T^{(0)}_{\alpha\beta} + \epsilon\sigma T^{(\sigma)}_{\alpha\beta} + \mathcal{O}(\epsilon^2)$:

$$T^{(0)\alpha\beta}(x) = \int d\tau \frac{\delta^4(x^\mu - z^\mu(\tau))}{\sqrt{-g}} u^\alpha(\tau) u^\beta(\tau),$$

$$T^{(\sigma)\alpha\beta}(x) = \int d\tau \nabla_\delta \left(\frac{\delta^4(x^\mu - z^\mu(\tau))}{\sqrt{-g}} \right) u^{(\alpha}(\tau) \tilde{S}^{\beta)\delta}(\tau) \,.$$

where $S^{\gamma\delta}$ is the spin tensor for the secondary. In the following we have chose a spin-supplementary condition, and linearise in the spin of the secondary.

The equations of motion become the self-forced Mathisson-Papapetrou-Dixon (MPD) equations of motion:

$$u^\beta \nabla_\beta u^\alpha = F^\alpha_{self-force}[h^R; z] - \frac{1}{2} R^\alpha{}_{\beta\gamma\delta} u^\beta S^{\gamma\delta}$$

$$u^\beta \nabla_\beta S^{\gamma\delta} = \tau^{\gamma\delta}_{self-torque}[h^R; z]$$

We solved the field equations, computed the flux and local force, and derived the balance law, in Phys. Rev. D 102, 064013, arXiv:1912.09461

Spinning secondary results

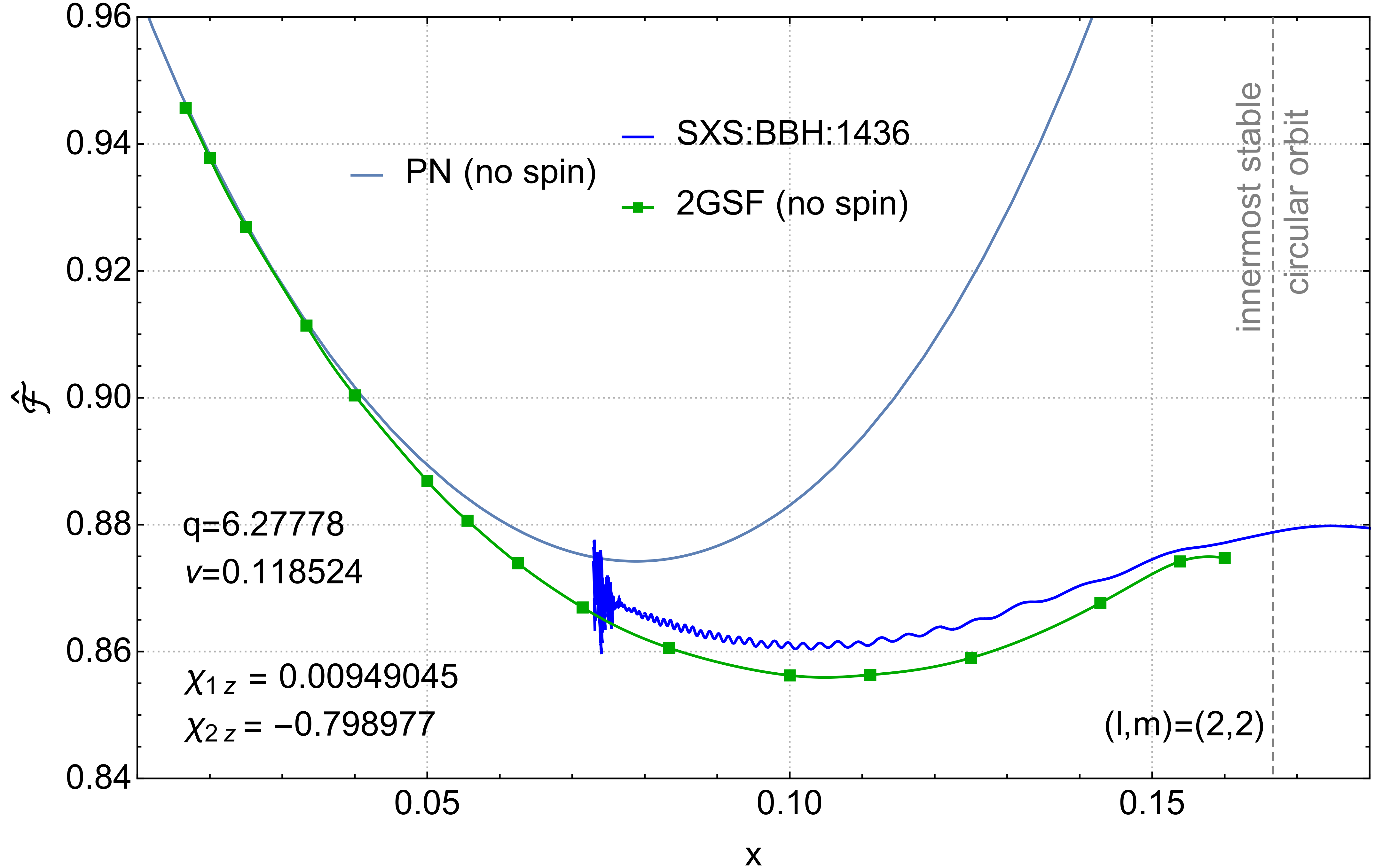

Spinning secondary results

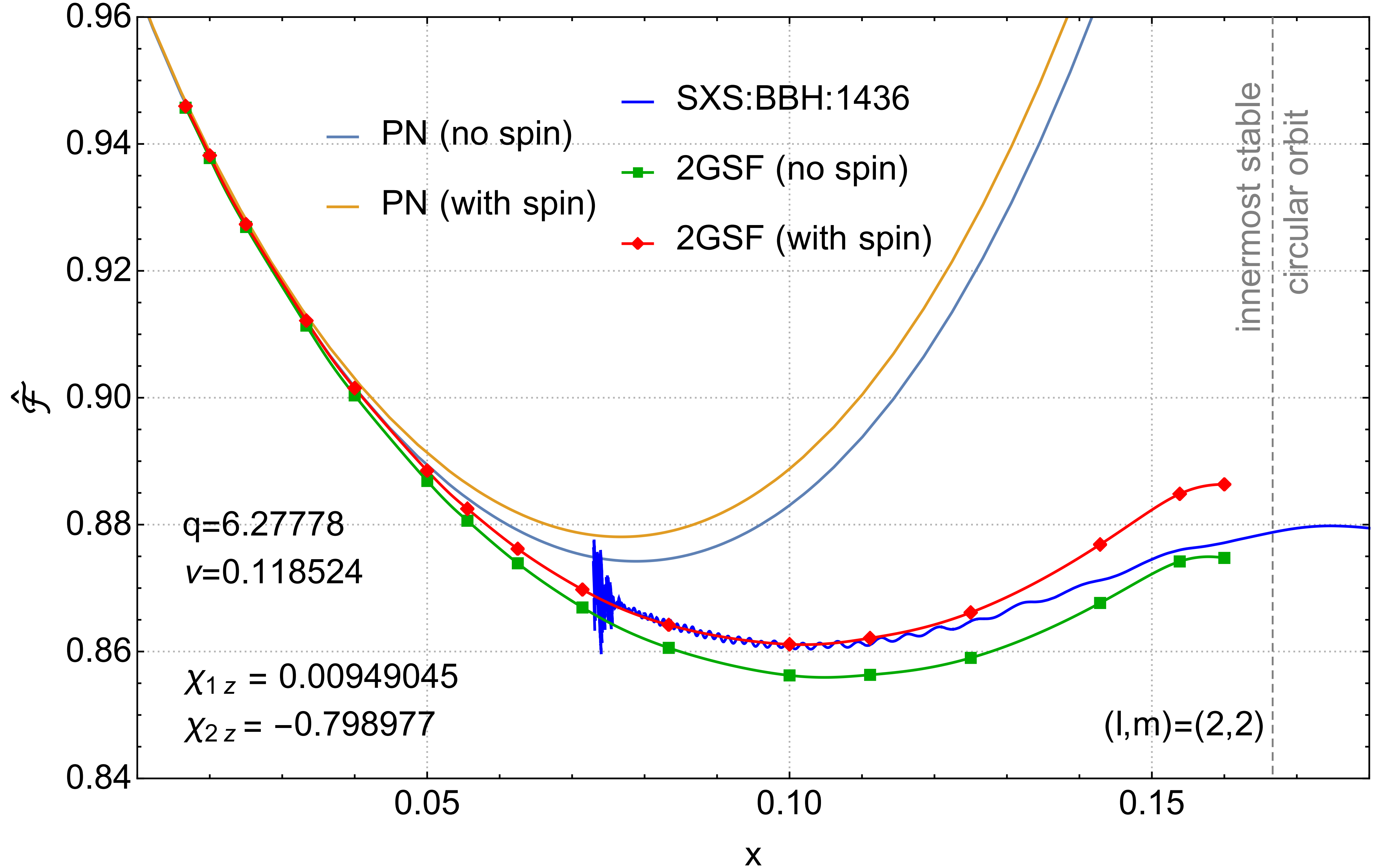

Adding the spin-flux from arXiv:1912.09461 we again see nice agreement with an NR waveform even at q=6.3

Summary

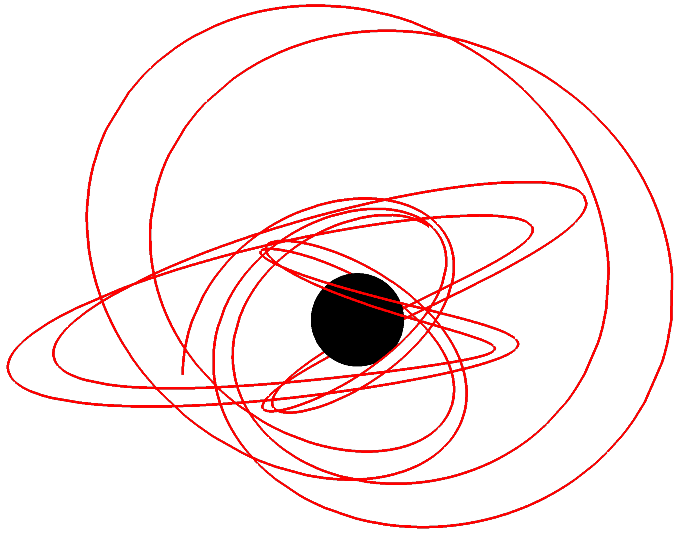

- We will observe many more small mass-ratio binaries with future GW detectors
- We need good waveform models for these binaries
- It looks promising that (second-order) perturbation theory can model binaries up to $q \sim 10$ (at least when the primary is not spinning and the orbit is circular)
- Future work: the waveform (which we will compute in milliseconds)

For further details on 2GSF see: arXiv:1201.5089, arXiv:1206.6538, arXiv:1311.3104, arXiv:1404.1543, arXiv:1505.07841, arXiv:1510.05172, arXiv:1608.06783, arXiv:1703.02836, arXiv:1908.07419; details on spinning flux: arXiv:1912.09461